Climate and Anthropogenic Impacts on North American Erosion and Sediment Transport since the Last Glacial Maximum: Evidence from the Detrital Zircon Record of the Lower Mississippi Valley

Nikki Neubeck[1], Andrew Carter[2], Tammy Rittenour[3], and Peter D. Clift[1]

1- Department of Geology and Geophysics, Louisiana State University, Baton Rouge, Louisiana 70803, USA

2- Department of Earth and Planetary Sciences, Birkbeck College, University of London, London WC1E 7HX, UK

3- Department of Geosciences, Utah State University, Logan UT 84322-4505

ABSTRACT

The Mississippi River provides an opportunity to examine models of sediment transport in large alluviated floodplain systems. We test the idea that sources of sandy sediment in such settings are invariable on timescales <10^4 y because of storage and recycling in the floodplains. To reconstruct the development of the Mississippi sediment load over the past 2500 years we collected sediment from an abandoned point bar complex nearby at False River, Louisiana. We also took annual samples from the lower reaches between 2015 and 2021 to assess changes on that timescale. Optically stimulated luminescence (OSL) dating indicated that the point bar accreted between 2460 and 860 years ago (a). Detrital zircon U-

Pb dating was used to assess sediment source and variability over time. We confirm a dominant sediment flux from the Rocky Mountain foreland but with higher relative erosion from the Superior Province during the Last Glacial Maximum (LGM) based on existing data from the Gulf of Mexico. There have been resolvable changes in the sources of sediment particularly since the LGM and after 860 a, but also over shorter, even sub-annual timescales in the recent past. These changes may reflect seasonal weather or storm events in the headwater regions and imply limited floodplain buffering of the sand load. In recent times this may reflect the installation of levees in the lower reaches, suppressing reworking. Changes over 10^2–10^3 y time periods may be related to changes in climate (e.g., the Mediaeval and Roman warm periods) and to the development of agriculture across North America after ~2000 a. Detrital zircon dating is an effective provenance tool and does not appear to be strongly biased by the grain size of the sediment in this setting.

Keywords: Erosion, Provenance, Zircon, Holocene, Sediment Transport

1. INTRODUCTION

Changes in regional climate within continental drainage basins have had major impacts on the rates and patterns of erosion in sediment source regions (Herman and Champagnac, 2016; Huntington et al., 2006). As a result, the origin of sediment that is delivered to the lower reaches of major catchment systems varies through time. Although tectonic processes in mountain sources, rejuvenating or diminishing source terrains and so impacting erosion patterns, climate-modulated surface processes also play a key role. Such influences can vary over orbital and shorter timescales ($<10^5$ y)(Clift et al., 2010; Colin et al., 2010; Fildani et al., 2016; Mason et al.,

2019). The impact that climate has on sediment production can be assessed if we examine the erosional response of a drainage basin over millennial or shorter timescales ($<10^4$ y) when tectonic processes are less likely to have impacted erosion patterns in large drainage systems. This contrasts with the possible influence of individual earthquakes on smaller catchments with restricted flood plains (Koi et al., 2008; Pearce and Watson, 1986). In this study we focus on the erosional record of the Mississippi River, the dominant catchment of the North American continent to see how climate change may have affected sediment production and transport in the Late Holocene (Fig. 1). We ask whether climate change affected erosion patterns and whether such changes were transmitted to the lower reaches.

North America has undergone significant climate changes since the Last Glacial Maximum (LGM: ~20 ka)(Aharon et al., 2012; Jackson et al., 2000; Quirk et al., 2020) and it might therefore be expected that the patterns of erosion and drainage would change as the glaciers retreated, the climate warmed and precipitation changed in intensity and location (Fildani et al., 2018; Oster et al., 2019). In addition, since the LGM, North America has been heavily settled (Lothrop et al., 2016; Waters, 2019). Agriculture with its associated deforestation and soil erosion, may have changed the patterns of erosion supplying sediment to the Mississippi River (Montgomery, 2007a). Furthermore, in the 20th Century the sediment flux through the river has been disrupted by the installation of major dams (Heimann et al., 2011; Thomson et al., 2022) and construction of levees (Syvitski et al., 2005).

Storage and recycling of sediment in major river floodplains has been invoked as a process that buffers variations in the composition and volumes of river sediment in large catchments, such as the Mississippi River basin (Bentley et al., 2015; Castelltort and Driessche, 2003; Romans et al., 2016). Allen (2008) suggested that landscapes can either be reactive, when

changes in erosion are transmitted to and preserved in depocenters, or buffered, in which erosional signals are lost during transport. If that is true the sediment reaching the ocean should not change substantially in its provenance over sub-tectonic time periods ($<10^6$ y) (Jerolmack and Paola, 2010). However, zircon U-Pb dating, which is commonly used to define provenance of siliciclastic sediment, reveals changes in sand composition during glacial cycles in the delta of the Indus (Clift et al., 2008), as well as changing proportions of sediment supply from the Andes versus the Amazon Craton in the modern Amazon Fan and lower river (Mason et al., 2019). Such variations in major fluvial systems have been tied to changing hydroclimate, with sea level controlling final delivery to the deep sea. It is possible for a drainage system to be buffered over long periods but reactive on shorter timescales.

It is clear that fine grained suspended sediment is not buffered over $10–10^4$ y periods. Fildani et al. (2018) identified variations in Mississippi Fan sediments that mirrored climatic trends during the last couple of glacial cycles in North America. Plastics and pollutants have been identified in deep-sea fan sediments offshore California where there is a close coupling between erosion onshore and sedimentation (Gwiazda et al., 2015). Hessler and Fildani (2019) make a strong case for coupling of continental erosion and sedimentation on deep-sea fans on millennial and shorter timescales, implying little buffering, but much of this evidence is from suspended fine-grained sediments and in drainages with short flood plains and/or narrow continental shelves.

In this study we test whether sandy sediment may be buffered in onshore drainage system with long floodplains on $<10^3$ y timescales by sampling the lower reaches of the Mississippi. We sample the modern channel, over time periods of years, as well as over hundreds of years using

cores taken within a late Holocene point bar complex located just north of Baton Rouge, Louisiana (Fig. 1).

By collecting multiple samples from the Mississippi River in a similar location over a span of less than a decade we also test the hypothesis that the commonly applied detrital zircon (DZ) U-Pb dating provenance method can reliably be used for constraining temporal changes in the source of sediment (Gehrels, 2014). The Mississippi was one of the first rivers to have its DZ signature analyzed, in an attempt to look at the long-term evolution of the continental crust (Iizuka et al., 2005). These same data can be used to look at sediment transport processes. If the river is undergoing significant buffering and recycling of sediment then similar DZ age populations might be expected in the lower reaches over periods of several years. Furthermore, the modern river DZ signature is important in the interpretation of the older geological record. Provenance studies often employ modern river compositions to compare with ancient sedimentary archives on continental margins to understand how a given drainage basin has evolved (Blum et al., 2017; Fildani et al., 2018). This approach becomes much more complicated if the sediment in the modern river is undergoing short-term changes that renders the composition of the river unrepresentative for use in geological interpretations (Hu et al., 2013; Thomson et al., 2022).

2. PREVIOUS WORK

2.1 Earlier Provenance Work

The sediment in the lower Mississippi River has been the subject of earlier provenance studies, including those employing the DZ method that we focus on in this study. Previous research of the modern Mississippi based on gauging data and suspended sediment

measurements implies that much of the sediment is derived from the Missouri River (56.9 Mt/yr, 40.5% of total), while the largest portion of the modern water discharge is from the Ohio River (8000 m^3/s compared to 2400 m^3/s in the Missouri River)(Meade and Moody, 2010). Mason et al. (2017) used DZ data and mixing models to estimate a "negligible" contribution from the Ohio River to the Mississippi Fan during the LGM (Fildani et al., 2016), compared with an estimated 14–17% Ohio River contribution to the modern lower Mississippi River, also based on DZ mixing models. That study estimated flux from the Missouri River of 59–67% net flux to the ocean. More recently Gregory et al. (2022) used DZ mixture models to estimate ~5% of the sediment in the lower reaches being derived from the Ohio River, but with 34% and 31% coming from the Missouri and Upper Mississippi respectively.

It is apparent that different studies derive different estimates for competing source contributions. It is not clear from these contrasting studies whether these different estimates represent real temporal changes in the composition of the river due to different sampling places and times. Changes in provenance spanning years or decades could be caused by the cut off of tributaries, such as the Red River following installation of the Old River Control Structure. This is a system of locks and floodgates that separates the Mississippi mainstream from the Atchafalaya River in southern Louisiana (Fig.1B). Alternatively, they might represent pulses of different compositions flowing through the mainstream in the wake of changing erosion upstream over short timescales, and not eliminated by buffering in the floodplains or anthropogenic effects.

3. BACKGROUND

3.1 Suspended load versus bedload

The speed of sediment transport is critical when trying to understand how quickly the river composition downstream of a confluence changes when sediment supply from that tributary is disrupted. The speed of transport of zircon sand grains is critical for the interpretation of the changing DZ record. There has often been the assumption that zircon grains are transported in the bedload when they are sand-sized because this mineral is especially dense (4.6 g/cm^3 compared to 2.65 g/cm^3 for quartz). As a result, zircon grains would travel more slowly than suspended sediment. Studies of DZ U-Pb ages in the Mississippi show response times to environmental forcing of $10^{3–4}$ y (Fildani et al., 2016; Mason et al., 2017), implying transport times of $10^{3–4}$ y. This contrasts with predictions based on the strong sediment buffering expected in long alluviated rivers (Castelltort and Driessche, 2003; Paola et al., 1992). We anticipate that suspended sediment could change on short time periods (days or weeks) because of weather events in the headwaters compared to the bedload. Such events could include major storms in limited parts of the basin or longer-lasting seasonal floods related to precipitation. The bedload is more susceptible to buffering either because of erosion of the channel base, or because of meandering. Either of these processes might dilute erosional pulses from upstream, potentially with sediments of contrasting DZ character.

3.2 Anthropogenic Influences

The amount of recycling in the lower reaches of the Mississippi Valley has reduced substantially because of engineering of the river for commercial purposes. The first levees were installed around New Orleans during the early 18th century to prevent flooding of the alluvial valley. The extension of these upstream was closely linked to intensifying economic activity, so

that it was not until the late 19th century that the river was heavily leveed as far upstream as the Arkansas River confluence (URS Group, 2012; US Army Corps of Engineers, 2017) (Fig. 1). Nonetheless, over the last couple of centuries the ability of the Mississippi to recycle its floodplain has been substantially curtailed because the levees prevent meander migration that rework the flood plains and can be a significant source of sediment is unconfined systems (Dingle et al., 2019; Mertes et al., 1996). As a result we might expect changes in sediment supply from the upper reaches to be more likely to be transmitted to the lower reaches of the river in modern times, as the recycling effect reduced. While many processes can cause changes in DZ spectra of sediments, on modern river systems the most significant drivers of sediment compositional changes are climate and anthropogenic forcing. Single large weather events, such as major storms, could theoretically produce and propagate erosional pulses through the river that would be recognizable in the lower reaches (Eden and Page, 1998; Jung et al., 2012). Alternatively, sediment mixing and buffering during transport might make it only possible to identify changes in the sediment supply caused by processes operating over longer timescales (100 or 1000's of years). Climatic episodes like the Little Ice Age or Mediaeval Warm Period that affected the Northern Hemisphere (Cronin et al., 2003) may produce long-term large-scale changes in river composition that are resolvable from the anthropogenic impacts noted above.

The construction of levees and dams along the Mississippi represents only the most recent phase of human disruption to this river system. Although humans first arrived in North America by at least 23 ka (Ardelean et al., 2020; Becerra-Valdivia and Higham, 2020; Bennett et al., 2020) the landscape was not radically impacted by their presence until more recently (Delcourt and Delcourt, 2004). Archaeologists suggest that there was a transition from a hunter-gatherer dominated society to a more agriculturally based one starting around 1000 y BP during

the Woodland Period (Delcourt and Delcourt, 2004). The tendency of humans to cut down forests and cultivate the topsoil, thus promoting its erosion, was accelerated following the European settlement of North America (Montgomery, 2007a). Here we investigate whether the effect of that transition is detectable in the sediment deposited in the lower reaches.

3.3 History of False River Point Bar

In this study we exploit the record preserved in a Holocene point bar complex located just downstream of the Old River Control Structure. This meander was cut off leaving a well-developed oxbow lake called False River (Figs. 1b and 2). The sediments preserved in the point bar represent the older deposits (pre-levee) of the Mississippi River in the lower reaches. Modelling and observations of meander migration rates from other large systems (Sternberg, 1956) suggest that the False River meander might have formed over 1000–1500 years. The timing of the initial cut-off of the False River point bar is estimated to be around 1720 CE (302 years ago), a date determined through aerial imagery and analysis of 18th Century maps (Fisk, 1947; Saucier, 1969). False River has been studied as an archetypal meandering river point bar and a survey of the topography mapped by LiDAR allows its migration history to be reconstructed, with re-orientation surfaces separating distinct phases of more gradual migration (Clift et al., 2019)(Fig. 2). The point bar complex provides the opportunity to sample Mississippi River sediment spanning a significant period (>1000 years). Sediment towards the base of the point bar section (>15 m) is coarser grained and more representative of sediment carried in the bedload in the channel thalweg (Allen, 1970; Smith, 1987). In contrast, sediment in the shallower levels is more likely to have been deposited from suspended sediment, either on natural levees banks of the river, or as an over-bank deposit during flooding events after the meander had

migrated from this area (Miall, 1985). Although the shallowest sediment could be overbank deposits, and potentially much younger than the underlying material. such deposits thin rapidly away from the channel. Because our coring penetrated around 5 m we believe that the material analyzed is not a distal floodplain sediment but must represent either the point bar itself, or sediment overlying this, but deposited close to the channel, soon after deposition of the underlying sequences. By limiting our coring to areas with well-developed scroll bar topography we can exclude the possibility that the material is much younger and deposited in cut-off shoots.

4. SAMPLING STRATEGY

In order to address our objective of assessing the relative stability of Mississippi sediment composition over annual time scales we repeatedly sampled the mainstream at Reserve, Louisiana (Fig. 1b; Table 1) from 2015 to 2021 in order to see if there was variation in the source of sediment to the lower reaches over timescales of years. Samples from the modern river were taken on foot directly from the bed of the active channel immediately next to the river bank, and not from older or suspended sediments. We were unable to sample the river during the spring because the high floodwaters at that time submerge the actively transporting sediments on the edge of the channel.

We further sampled older river sediments by taking cores from the False River point bar (Locations in Table 1). Because this is understood to have been cut off in ~1720 CE (Fisk, 1947; Saucier, 1969) and to have a projected timeframe of active accretion of around 1000–1500 years this gave us the opportunity to look at how the river evolved over approximately the last 2000 years and to see whether it has been stable in source over that time. We took samples from

existing cores acquired in an earlier study focused on grain size analysis (Clift et al., 2019). We mostly took samples from shallower stratigraphic levels, the top 5 m, which would be equivalent to sediment deposited close to the riverbank in the modern day. In doing so we aim to compare similar sediments from the Recent and Holocene. Although some of the coarser point bar sediments may be more transported as bedload our aim was to mostly compare similar materials so that any transport-related lag times would be comparable.

We also performed coring using a *Geoprobe* MC5 geotechnical coring machine. We penetrated 5 m into the sub-surface to avoid sampling material influenced by agricultural activities. We penetrated deep enough (~5 m) to sample the muddy bar top, typically 3–5 m thick in this area, based on earlier coring (Clift et al., 2019), but not the underlying inclined heterolithic strata (Ghinassi et al., 2016; Thomas et al., 1987). Coring was undertaken using 2.5 m-long plastic core liners, painted black to prevent resetting by sunlight that would disturb optically stimulated luminescence (OSL) dating.

This new round of sampling allows us to directly link depositional age constraints with the provenance of the sediment at that time, thus allowing a relatively detailed reconstruction of the river composition on centennial timescales over the past few thousand years to be achieved. Sediments deposited deeper in the point bar are necessarily older than those in the shallow parts in the same location. The rate of propagation of the point bar means that this vertical offset does not introduce a very high uncertainty (± ~32 years on average, assuming 7° dip and 1600 years (see below) to migrate 12 km across the entire point bar; average 7.5 m of meander migration per year). By coring across the whole point bar, we were able to determine the time span of sedimentation of this complex, with the age of individual samples derived by linear extrapolation

between the points where depositional ages were available and considering the major re-orientation surfaces that define the accretion history of the point bar.

5. ANALYTICAL METHODS

5.1 Optically Stimulated Luminescence

We employ the OSL dating technique because the sediments in the point bar do not contain organic material or charcoal for radiocarbon dating. Holocene deposits are ideal for this method. OSL dating provides an age estimate of sediment deposition by dating the last exposure to sunlight or heat of siliciclastic sediment, which is assumed to be during sediment transport (Rittenour, 2018). Following burial, exposure to ionizing radiation from the surrounding sediments and cosmic rays leads to the accumulation of trapped charge (free electrons) in defects in the crystal-lattice structure of the target mineral, quartz in this case. These trapped charges produce luminescence (photons of light) when stimulated by controlled light in the laboratory. The intensity of the luminescence signal is related to the radioactivity of the depositional environment and duration of burial (i.e. the age of last exposure to light or heat) (Rhodes, 2011).

Seven samples were processed at the Luminescence Laboratory at Utah State University for OSL analysis. Full analytical details are provided in the online supplement in the Data Repository and summarized in Table 2.

5.2 Grain Size

We measured the grain size of the sediments analyzed for DZ to understand the potential role that grain size has in impacting our assessment of the provenance. A total of twenty-five samples from both the False River point bar and the modern river were analyzed following the procedure of Hülse et al. (2012). The samples were analyzed for grain size distributions using a Beckman-Coulter (LS 13-320SW) Laser Diffraction Particle Size Analyzer at Louisiana State University (LSU). Grain size results are shown in Table S1. Full analytical details are provided in the online supplement in the Data Repository.

5.3 Geochemical Analysis

X-Ray Fluorescence (XRF) analysis was completed at LSU with samples analyzed on a PANalytical Epsilon3^{XLE} energy dispersive XRF spectrometer at the LSU Shared Instrumentation Facility. Three standards, USGS MAG-1 (Marine Sediment), GSJ JSd-1 (Stream Sediment), and GSJ JSl-1 (Slate) were analyzed in triplicate as unknowns at the beginning and end of each analytical session to check the accuracy of the calibration and to monitor for instrumental drift. XRF results of the analysis are provided in Table 3. Analytical uncertainty for major elements was ±5%. Full analytical details are provided in the Data Repository.

5.4 Zircon U-Pb Geochronology

Zircons were separated from the bulk samples at GeoSep Services Inc. in Moscow, Idaho using a form of standard heavy mineral separating methods (Donelick et al., 2005). A total of seven mounts were analyzed at the London Geochronology Centre and two at Washington State University. DZ U-Pb age results are provided in Table S2. Data are available through the Mendeley Database and from the Geochron database at University of Arizona. Full analytical details are provided in the Data Repository supplement.

The DZ method is based on the idea that sediments carried by the Mississippi River are derived from the various contrasting basement terrains that form the North American continent (Fig. 3), and whose geology is summarized in the Data Repository. Their unique individual histories and compositions make it possible to resolve from where the sediment is derived. Zircon ages of North American source terrains are well known (Gehrels, 2014; Laskowski et al., 2013), but interpretation of zircon data can be complicated because of sediment reworking during transport and deposition, as well as uplift and erosion of older sedimentary rocks (Romans et al., 2016). Furthermore, variable fertility of zircon grains in different sources can complicate data interpretation (Blum and Pecha, 2014).

6. RESULTS

6.1 Optically Stimulated Luminescence

Seven OSL ages were collected (Table 2). Ages span from 860 to 2460 a, spanning ~1600 y and overlapping the Mediaeval and Roman Warm Periods (950 CE to 1250 CE and 250 BCE to CE 400 respectively), as well as the intervening cooler Dark Ages interval (400 CE to

950 CE). Uncertainties in the OSL ages are on the order of 100–300 years, but the dating indicates that the meander scrollbars formed between the Roman and Medieval Warm periods. As a result, correlation with existing climate records is possible. By measuring the distance perpendicular to the scrollbar topography between different dated points it is possible to estimate the rate of migration of the meander through time. Total distance of 10.6 km from the oldest dated point and the terminal apex yields and average rate of 6.6 m/y. The fastest rates recorded are in the oldest part of the point bar where the apex was moving at around 20 m/y, although the uncertainties are great and could be as slow as 1.4 m/y (Table 2). After that time the average rates vary between 7.0 and 2.1 m/y until around 1000 y BP, possibly as slow as 0.68 m/y between 1690 and 1500 a. The slowest average rate of migration occurred after deposition of the youngest of our data points and the historical cut-off in 1720 when the rate of migration was only around 1 m/y (0.75–1.35 m/y).

6.2 Grain size

The range of grain sizes measured from the samples is shown in Figure S1. There is a well-developed peak for each grain size spectrum, with only a few samples not showing a relatively high degree of kurtosis, indicating mostly good sorting. Many of the sediments show a positive skew, with a long tail of coarser material. The False River core samples taken from deep (>5 m) within the point bar complex are dominated by fine sand (B2-14/B2-16, W1-17/W1-18, W2-5, W3-10/W3-11, W3-18, J2-10/J2-11), with a minority of medium sand, while the remaining shallower samples are dominated by silt and very fine sand. Samples from the modern Mississippi River are dominantly of fine sand, and also show positive skew. A smaller number of

329 samples from the modern river also contain significant amounts of silt and very fine sand
330 (Samples BLBR21, 21022001, 20110101).
331
332 **6.3 Major Element Compositions**
333 Sediments considered in this study span a wide range of major element compositions.
334 SiO_2 percentages range from 56.2% to 86.8%, while Al_2O_3 ranges from 3.5% to 16.9%. Much of
335 the variability can be attributed to grain size, with muddier samples typically showing lower
336 SiO_2 (Fig. 4A). Loss on ignition (LOI) can be significant, ranging up to 14.9%. Sediments with
337 high LOIs typically show low SiO_2 reflecting their muddy lithology and generally more
338 weathered state. We can assess the overall geochemical character of the sediments using an array
339 of major element discrimination diagrams in order to assess the overall character.
340 The ternary CN-A-K diagram of Fedo et al. (1995)(Fig. 5) can be used to understand the
341 degree of chemical weathering. There is a wide range of compositions found in the lower
342 Mississippi and the False River point bar. The sediments form an array trending towards the illite
343 end member in the top right-hand part of this diagram, indicating progressively more chemical
344 weathering towards this clay mineral. The point bar sediments generally show higher degrees of
345 alteration (Chemical Index of Alteration) compared to sediments in the modern Mississippi and
346 major tributaries, with the exception of the Ohio River sample which, shows more chemical
347 weathering than other tributaries (Table 3). There is a modest preference for the most altered
348 sediments to be the youngest.
349 The overall character of the sediment can be revealed through the discrimination diagram
350 of Herron (1988) based on SiO_2, K_2O, Fe_2O_3 and Al_2O_3 contents (Fig. S2A). Again, the
351 sediments show an array with more sediments from the point bar plotting within the general field

of litharenite and wackes, while many of the sediments from the modern river are defined as being subarkose based on the Herron (1988) scheme. Only two sediment samples (20092401 and 20110101) qualify as quartz arenites, the most compositionally mature variety.

The major element analysis is not useful for defining provenance because it is too dependent on grain size and chemical weathering (Lupker et al., 2012). The discrimination diagram of Singh et al. (2005) to understand how the different sediments have been affected by transport and hydrodynamic sorting. All the sediment samples are displaced towards lower values of Al_2O_3/SiO_2 and Fe_2O_3/SiO_2 compared to the upper continental crust (UCC) average (Fig. S2B), indicative of quartz enrichment due to sorting. We do not consider the major element compositions further.

6.4 Zircon U-Pb Ages

The range of DZ U-Pb ages acquired from the samples are shown in Figure 6 as a kernel density estimate (KDE) diagram (Vermeesch, 2018). All the samples show several common populations. Prominent populations include <100 Ma, 200–100 Ma, 1200–900 Ma, 1500–1300 Ma, and 1800–1600 Ma. Smaller populations are also noted between 350 and 650 Ma, as well as around 2700–2500 Ma. Many of these populations correlate with the basement ages summarized above (Fig. S3).

7. DISCUSSION

We now consider the implications of the zircon age data from the three different populations, i.e., the modern river, the late Holocene sediments from the point bar as well as existing data from the submarine fan dating from the LGM. We first consider potential complications in the interpretation of the age data and how these might affect the interpretation of similar data sets in other places. We then talk about temporal evolution of erosion in the Mississippi Basin, and what might have influenced that. Finally, we discuss what these data mean for the transport of sediment through the river system and what processes have affected that since the LGM, especially anthropogenic effects.

7.1 Detrital Zircon U-Pb Age Distributions

The KDE diagrams (Fig. 6) reflect the varied sources that contribute to the Holocene and recent Mississippi River. We see major contributions to all of the sediments from zircons typical of erosion from the Cordillera (<200 Ma), from the Grenville Province (1200–900 Ma) and also the Yavapai-Mazatzal Province (1800–1600 Ma)(Fig. S3). Smaller populations are associated with DZ age ranges linked to the Taconic (500–350 Ma), Peri-Gondwanan (650–500 Ma), Trans-Hudson (2200–1800 Ma) and Superior provinces (2700–2500 Ma). Although many of the sediment sample DZ U-Pb age distributions share similarities there are significant differences in the relative proportion of the different populations that are derived from these different sources. The variable proportions of U-Pb population reflect changing patterns of erosion and sediment supply over different time scales. There is no clear temporal evolution visible based on this analysis.

DZ samples with a large number of grains dated (>200) allow smaller age fractions to be identified and may be more useful in identifying the source contribution compared to DZ

397 samples with the minimum number of grains dated (Pullen et al., 2014). In order to assess
398 whether our sample size might be affecting our provenance conclusions, we analyzed three
399 samples in two stages, initially with a moderate number of grains (Vermeesch, 2004) and then
400 with enlarged data set. Figure S4A shows the KDE plots for these repeat analyses. Minor
401 differences are noted between the large and small datasets, but the overall character remains the
402 same in that the same populations are present and there is no major change in the relative
403 proportion of U-Pb age populations with a larger number of grains dated.

404 We further examine whether the DZ method might be susceptible to the influence of grain
405 size given the range of sediments considered in the study.There is a slight tendency to higher Zr
406 concentrations (a proxy for zircon abundance) in finer grained sediments, (<100 μm) compared
407 to coarser material, although there is substantial scatter, and some fine-grained material is also
408 poor in zircon (Fig. 4B). We compare median grain size with provenance-sensitive age
409 populations to see if grain size introduces bias. It is possible that certain sources preferentially
410 supply coarser or finer material, being susceptible to hydrodynamic sorting which could bias DZ
411 U-Pb age distributions. Figure 7 however shows that this is likely not the case. There is no clear
412 relationship between the abundance of grains of any given age population being closely
413 correlated with its median grain size and this gives us confidence that sediments spanning a
414 range of grain sizes can be equally representative of the material being transported in the river at
415 the time of its deposition.

416 We attempt an objective assessment of how these sediments relate to each other and the
417 contributing source regions or tributaries using a multi-dimensional scalar (MDS) diagram made
418 with the *Provenance R* package of Vermeesch (2013). This analysis compares the different

spectra of the DZ ages using a Kuiper statistical test and spatially plots them on dimensionless axes, similar to a principal component analysis plot. Sediments with similar DZ age spectra plot close together on the diagram.

In order to see whether the small and large sample sets were statistically different, as has been suggested (Pullen et al., 2014), we compared them with basement ages compiled with the literature (Fig. S3B; see Data Repository for the source compilation details). This analysis shows that the variability between small and large data sets is small compared to the overall range of the various sources that are contributing to the lower reaches and we conclude that while smaller data sets are sub-optimal they do a reasonable job of reproducing the provenance, consistent with the earlier work of Vermeesch (2004).

Considering the sediment data sets and the tributary end members the MDS analysis shows a general clustering of sediments from the False River point bar (Fig. 8). This False River grouping coincides with some of the sediments in the modern lower reaches. One of the modern river samples (LA1701) plots far from all the other sediments, and represents an end member, with a particular contrast compared to the equally anomalous sample taken near Baton Rouge (BL_BR) by Blum et al. (2017). Sediments from the LGM in the Gulf of Mexico, analyzed by Fildani et al. (2016) plot separately from other Mississippi sediments, but very close to the composition of the modern Missouri River. The Ohio River is the least similar to any of the lower reach samples, implying that this tributary contributes little to the total zircon budget. The mixed sediments largely fall between samples from the Missouri and Upper Mississippi rivers, consistent with earlier models that imply the Missouri River to be the dominant supplier of material to the mainstream (Gregory et al., 2022; Mason et al., 2017). Nonetheless, the distribution requires input from all the major tributaries to account for the variability seen in the

MDS. These overall conclusions are further supported by inter-sample comparison by Kuiper testing, as described in the Data Repository.

7.2 Temporal Variations

We attempt to derive a more objective and quantitative estimate of the varying contributions from different source terrains to the sediments using a Monte Carlo-based statistical method, DZMix (Sundell and Saylor, 2017). In this approach we use the potential source region DZ U-Pb signatures already discussed and plotted above, as documented in the Data Repository. In each case 10,000 attempts are made to replicate a particular DZ age spectrum through varying the contributions from the various sources to match the observed zircon age spectrum, with the best 1% selected. This type of mixture modeling heavily depends on how well defined the source areas are, although in the case of the Mississippi River many of the sources are characterized by many DZ U-Pb distributions containing hundreds, if not thousands of individual grain ages.

Furthermore, there is the added complexity that material that was originally derived from one basement block might have been eroded and transported to form the sedimentary cover of a different block from where it is then reworked. Recycling material out of older sedimentary sequences complicates the sediment unmixing, especially from sedimentary terrains like the Rocky Mountain foreland. There is no simple, definitive way to remove the recycling effect, but it might be expected to influence all our samples. Instead, we look for systematic major changes in DZ populations to quantify changes in provenance with the understanding that even apparently unique DZ age peaks might be recycled from older sedimentary deposits. Although the unmixing method appears to be quite quantitative, it does not consider differences in zircon

fertility within different source units or influences of recycling and grain size due to hydrodynamic sorting and so it is best used in a general fashion to look at overall trends in the DZ age spectra.

The results of our unmixing calculations are presented in Table S3. The results are derived using three statistical tests: the Kuiper, the K-S test and the cross-correlation method as defined by Sundell and Saylor (2017). We prefer to use the Kuiper test as being widely accepted within the DZ community. A cumulative frequency plot is provided in the Online Supplement showing the best 1% of the models compared to the observed spectra to demonstrate how well each of the forward models compares with the sediment which it is trying to duplicate (Fig. S5). In general, attempts to unmix using modern tributary DZ data showed poorer matches and as a result we focus our discussion here on an unmixing assessment in relation to the major source terrains which provide better matches. This inability to derive satisfactory results from the tributary end members implies that either the modern tributaries are not well defined, or that they are variable over short time periods so that single grab samples from them are unsuitable as long-term proxies for their influence on the system.

7.2.1 Multi-Millennial Variations

The results of the unmixing calculations are shown as pie diagrams (Fig. S6) visualizing the relative contribution of the major different sources. There is significant variability in the sediments, although the Rocky Mountain foreland and Yavapai-Mazatzal blocks are the single greatest contributors to many of the sediments. Rocky Mountain foreland derived grains represent an average of 21.0% at the LGM. There is a major contribution (14.2–31.2%, mean 21.3%) to Mississippi Fan LGM sediments (Fildani et al., 2016) from the Superior Province (Fig.

9; Table S3) (Samples 621-9, 614-1 and PC-29). Erosion from the Appalachians was low at the LGM, accounting for an average of just 4.1 % of the total, while the Yavapai-Mazatal was also modest in supplying just 11.7% on average at this time.

There are significant differences between the source of sediment during the LGM compared to the late Holocene and subsequently with the composition of the river in the last 10 years (Figs. S6, S7 and 9). This observation shows that the river lower reaches are not fully buffered over multi-millennial timescales. Sedimentation in the deep-water Gulf of Mexico is restricted to glacial times when the sea level was lower. At that time the river was able to supply material directly into the deep water (Anderson et al., 2016; Bentley et al., 2015). During sea level highstands sediment is sequestered in the delta and on the shelf. When sea level is low the delta and continental shelf were incised and the deposits from the previous highstand would be reworked into the deep water, essentially diluting, or homogenizing any short-term signals. Thus, the deep-sea record is likely to be buffered over multi-millennial scales and the changes seen in the lower reaches would not be preserved in the rock record. Realizing that drainages can be buffered or not on different timescales blurs the boundaries between the buffered and reactive end members propounded by Allen (2008).

7.2.2 Centennial Variations

Compared to the LGM late Holocene sediments show reduced contributions from the Superior Province (average 12.3%; Fig. 9) and from the Rocky Mountain foreland (average 17.5%) in the Late Holocene. Yavapai-Mazatal erosion peaked (21.2%) in the late Holocene.

Supply from the Appalachians was variable in the late Holocene (0.86–2.46 ka), but reached maximum values (average 7.2%) from this source, approximately correlating with the Roman Warm Period (250 BCE to CE 400, 1622–2272 a).

Prior to around 2000 a most inhabitants of North America employed hunter-gatherer economies (Delcourt and Delcourt, 2004), but during the Woodland Period (1000 BCE–1000 CE, 1022–3022 a) there was a transition to greater reliance on agriculture and the development of settled communities (Anderson et al., 2002). It has been documented that ploughing of soil and removal of forest has resulted in enhanced soil erosion worldwide (Montgomery, 2007a), which increases the total amount of sediment in the rivers (Syvitski et al., 2005). Our preferred interpretation is that the relative increases seen in sediment production from the Appalachians and Yavapai-Mazatzal during the late Holocene, and which broadly correlate with the Woodland Period, may reflect this change in land use across wide areas of the Mississippi catchment (Fig. 10).

The scatter in the erosional contribution in the Late Holocene samples indicates incomplete buffering of sedimentation at the time. As a result, it should be possible to correlate changes in sediment compositions in the delta with anthropogenic or climatic events in the headwaters if they were sufficiently strong as to alter the provenance of the river.

7.2.3 Annual Variations

Superior Province contributions to the modern river are the lowest for any of the age groups (11.3% between 2015 and 2021), and the Appalachian contribution is also modest,

reaching an average of just 5.3%. In contrast, Rocky Mountain foreland grains represent a large population (27.1%) in the modern river, partly at the expense of reduced erosion from the Yavapai-Mazatal (average 16.4%).

We lack samples between the late Holocene and the modern to say when the transition to less erosion from the Appalachians and more erosion from the Rocky Mountain foreland occurred, although it is possible that it coincided with the spread of European settlement across the Great Plains, which might be expected have increased the amount of erosion from the foreland (Montgomery, 2007a; Montgomery, 2007b). In more recent years forests have largely regrown through much of the Appalachians, which in turn would favor development of new soils and fixing of eroded material in place, reducing the amount of flux into the river from that area (Fig. 10). Although damming has reduced total sediment flux to the lower reaches there is no reason to believe that this disproportionately affects one part of the catchment more than others and would not affect provenance proxy records.

Variability in the modern river indicates that the river is not fully buffered on an annual basis. Statistically resolvable differences are presumably related to the supply of sediment from upstream, and in turn potentially reflect the effects of weather events in the upper reaches of the river, enhancing or reducing sediment supply from individual source areas. Our data imply that changing sediment supply from the upper reaches is not being entirely eliminated by storage and reworking in the lower reaches on annual time scales (Covault et al., 2013). The observation that the river is not completely buffered in the present day, despite flowing across a long alluviated floodplain, may reflect its highly engineered state, with at least the lower reaches of the river, as far upstream as the Ohio River confluence (~1600 km) being constrained within permanent

552 levees and therefore unable to meander as it would in the natural state. This reduces the chances
553 of storing sediment on, or recycling sediment from the floodplains.

554 The significant variability in the modern river implies that if geologists wish to compare
555 the composition of modern rivers with ancient deposits, then the river should be sampled on
556 several occasions in order to generate a robust average composition, rather than relying on a
557 random single sample. The significant differences between sediment sampled in different years
558 needs to be recognized when comparing modern with ancient sediments. Likewise, if ancient
559 sedimentary deposits are not sampled several times there will be some uncertainty regarding
560 whether these are truly representative of the system at the time of sedimentation, although this
561 study would suggest that the degree of variation should not be too significant.

562

563 ## 9. CONCLUSIONS

564 Analyses of detrital zircons in sediment samples taken in the lower Mississippi over annual
565 time-scales shows that the DZ U-Pb method is powerful in identifying changing sources of
566 sediment in large river systems. This study confirms earlier work that much of the sediment has
567 been derived from the Rocky Mountain foreland, although we identify significant changes in
568 source since the LGM. In glacial times the Superior Province was generating more of the
569 sediment than during the Holocene, probably because of strong glacial erosion and meltwater
570 run-off in the Great Lakes region. We further identify changes in the dominant sources between
571 around 860 years ago and 2015–2021. The Mississippi River is not entirely buffered in its
572 composition over at least the last seven years and we suggest that this is at least partly related to
573 short-term changes in erosion of crystalline bedrock, sedimentary rocks, or Quaternary deposits

in the headwaters and may have a reduced degree of recycling/storage of sediment in the floodplains, as a result of the extensive levee system. Sea level induced storage and then recycling of sediment over glacial cycles is however likely to result in strong buffering in the submarine fan over timescales of $>10^5$ y. Depending on the timescales the Mississippi may be both reactive and buffered. The modest buffering on shorter timescales means that care should be exercised when using modern river sediments as proxies for comparison with the ancient record. Whether the change of erosion away from the Superior Province and towards the Appalachians and Yavapai-Mazatzal in the late Holocene reflects the impact of human settlement is not clear since we do not have sufficient samples preceding and post-dating that time period. Nonetheless, the spread of agriculture and large-scale settlements, starting in the Woodland Period (~2000 a), may be influential in controlling the supply of sediment into the river since that time. The sediment in the modern Mississippi supports the idea that grain size is not a significant bias in estimating provenance, at least in North America.

ACKNOWLEDGEMENTS

This study was supported by funding from the Charles T. McCord Chair in Petroleum Geology at LSU. The authors want to thank Matthew Loocke for his assistance with XRF analysis and Paul O'Sullivan and colleagues at GeoSep services for their help with mineral separating and some U-Pb dating. We also thank Bill Gibson for his help with the Geoprobe. Kelly Thomson and an anonymous reviewer are thanked for helping improve the initial submission with their comments. Data for this paper are available from Mendeley Data at https://data.mendeley.com/datasets/trtnw8vx95/draft?a=4923e382-b53a-4f11-a36b-

14e61ca09ac1, and from the Geochron database at the University of Arizona (http://geochron.org/)

REFERENCES CITED

Aharon, P., Aldridge, D., and Hellstrom, J., 2012, Rainfall Variability and the Rise and Collapse of the Mississippian Chiefdoms: Evidence from a DeSoto Caverns Stalagmite, *in* Giosan, L., Fuller, D. Q., Nicoll, K., Flad, R. K., and Clift, P. D., eds., Climates, Landscapes, and Civilizations, Volume 198: Washington, D.C., AGU, p. 35-41.

Allen, J. R. L., 1970, Studies in fluviatile sedimentation: a comparison of fining-upwards cyclothems, with special reference to coarse-member composition and interpretation: Journal of Sedimentary Research, v. 40, no. 1, p. 298-323.

Allen, P. A., 2008, Time scales of tectonic landscapes and their sediment routing systems, *in* Gallagher, K., Jones, S. J., and Wainwright, J., eds., Landscape Evolution: Denudation, Climate and Tectonics over Different Time and Space Scales, Volume 296: London, Geological Society,, p. 7-28.

Anderson, D. G., Kidder, T. R., Watson, P. J., Rafferty, J., Herbert, J. M., and Peacock, E., 2002, The Woodland Southeast, The University of Alabama Press, 680 p.:

Anderson, J. B., Wallace, D. J., Simms, A. R., Rodriguez, A. B., Weight, R. W. R., and Taha, Z. P., 2016, Recycling sediments between source and sink during a eustatic cycle: Systems of late Quaternary northwestern Gulf of Mexico Basin: Earth-Science Reviews, v. 153, p. 111-138. doi:10.1016/j.earscirev.2015.10.014.

Ardelean, C. F., Becerra-Valdivia, L., Pedersen, M. W., Schwenninger, J.-L., Oviatt, C. G., Macías-Quintero, J. I., Arroyo-Cabrales, J., Sikora, M., Ocampo-Díaz, Y. Z. E., Rubio-Cisneros, I. I., Watling, J. G., de Medeiros, V. B., De Oliveira, P. E., Barba-Pingarón, L., Ortiz-Butrón, A., Blancas-Vázquez, J., Rivera-González, I., Solís-Rosales, C., Rodríguez-Ceja, M., Gandy, D. A., Navarro-Gutierrez, Z., De La Rosa-Díaz, J. J., Huerta-Arellano, V., Marroquín-Fernández, M. B., Martínez-Riojas, L. M., López-Jiménez, A., Higham, T., and Willerslev, E., 2020, Evidence of human occupation in Mexico around the Last Glacial Maximum: Nature, v. 584, no. 7819, p. 87-92. doi:10.1038/s41586-020-2509-0.

Becerra-Valdivia, L., and Higham, T., 2020, The timing and effect of the earliest human arrivals in North America: Nature, v. 584, no. 7819, p. 93-97. doi:10.1038/s41586-020-2491-6.

Bennett, M. R., Bustos, D., Odess, D., Urban, T. M., Lallensack, J. N., Budka, M., Santucci, V. L., Martinez, P., Wiseman, A. L. A., and Reynolds, S. C., 2020, Walking in mud: Remarkable Pleistocene human trackways from White Sands National Park (New Mexico): Quaternary Science Reviews, v. 249, p. 106610. doi:10.1016/j.quascirev.2020.106610.

Bentley, S. J., Blum, M. D., Maloney, J., Pond, L., and Paulsell, R., 2015, The Mississippi River source-to-sink system: Perspectives on tectonic, climatic, and anthropogenic influences, Miocene to Anthropocene: Earth-Science Reviews, v. 153, p. 139-174. doi:10.1016/j.earscirev.2015.11.001.

Blum, M., and Pecha, M., 2014, Mid-Cretaceous to Paleocene North American drainage reorganization from detrital zircons: Geology, v. 42, no. 7, p. 607-610. doi:10.1130/G35513.1.

Blum, M. D., Milliken, K. T., Pecha, M. A., Snedden, J. W., Frederick, B. C., and Galloway, W. E., 2017, Detrital-zircon records of Cenomanian, Paleocene, and Oligocene Gulf of Mexico drainage integration and sediment routing: Implications for scales of basin-floor fans: Geosphere, v. 13, no. 6, p. 2169-2205. 10.1130/ges01410.1.

643 Castelltort, S., and Driessche, J., 2003, How plausible are high-frequency sediment supply-
644 driven cycles in the stratigraphic record?: Sedimentary Geology, v. 157, p. 3-13.
645 doi:10.1016/S0037-0738(03)00066-6.
646 Clift, P. D., Giosan, L., Blusztajn, J., Campbell, I. H., Allen, C. M., Pringle, M., Tabrez, A.,
647 Danish, M., Rabbani, M. M., Carter, A., and Lückge, A., 2008, Holocene erosion of the
648 Lesser Himalaya triggered by intensified summer monsoon: Geology, v. 36, no. 1, p. 79–
649 82. doi: 10.1130/G24315A.1.
650 Clift, P. D., Giosan, L., Carter, A., Garzanti, E., Galy, V., Tabrez, A. R., Pringle, M., Campbell,
651 I. H., France-Lanord, C., Blusztajn, J., Allen, C., Alizai, A., Lückge, A., Danish, M., and
652 Rabbani, M. M., 2010, Monsoon control over erosion patterns in the Western Himalaya:
653 possible feed-backs into the tectonic evolution, *in* Clift, P. D., Tada, R., and Zheng, H.,
654 eds., Monsoon evolution and tectonic-climate linkage in Asia, Volume 342: London,
655 Geological Society, p. 181–213.
656 Clift, P. D., Olson, E. D., Lechnowskyj, A., Moran, M. G., Barbato, A., and Lorenzo, J. M.,
657 2019, Grain-size variability within a mega-scale point-bar system, False River,
658 Louisiana: Sedimentology, v. 66, no. 2, p. 408-434. doi:10.1111/sed.12528.
659 Colin, C., Siani, G., Sicre, M.-A., and Liu, Z., 2010, Impact of the East Asian monsoon rainfall
660 changes on the erosion of the Mekong River basin over the past 25,000 yr: Marine
661 Geology, v. 271, no. 1-2, p. 84-92. doi:10.1016/j.margeo.2010.01.013.
662 Covault, J. A., Craddock, W. H., Romans, B. W., Fildani, A., and Gosai, M., 2013, Spatial and
663 temporal variations in landscape evolution; historic and longer-term sediment flux
664 through global catchments: The Journal of Geology, v. 121, p. 35-56.
665 Cronin, T. M., Dwyer, G. S., Kamiya, T., Schwede, S., and Willard, D. A., 2003, Medieval
666 Warm Period, Little Ice Age and 20th century temperature variability from Chesapeake
667 Bay: Global and Planetary Change, v. 36, no. 1, p. 17-29. doi:10.1016/S0921-
668 8181(02)00161-3.
669 Delcourt, P. A., and Delcourt, H. R., 2004, Prehistoric Native Americans and ecological change,
670 Cambridge, Cambridge University Press, 221 p.:
671 Dingle, E. H., Paringit, E. C., Tolentino, P. L. M., Williams, R. D., Hoey, T. B., Barrett, B.,
672 Long, H., Smiley, C., and Stott, E., 2019, Decadal-scale morphological adjustment of a
673 lowland tropical river: Geomorphology, v. 333, p. 30-42.
674 doi:10.1016/j.geomorph.2019.01.022.
675 Donelick, R. A., O'Sullivan, P. B., and Ketcham, R. A., 2005, Apatite fission-track analysis:
676 Reviews in Mineralogy and Geochemistry, v. 58, no. 1, p. 49-94.
677 Eden, D. N., and Page, M. J., 1998, Palaeoclimatic implications of a storm erosion record from
678 late Holocene lake sediments, North Island, New Zealand: Palaeogeography,
679 Palaeoclimatology, Palaeoecology, v. 139, no. 1, p. 37-58. doi:10.1016/S0031-
680 0182(97)00136-3.
681 Fedo, C. M., Nesbitt, H. W., and Young, G. M., 1995, Unraveling the effects of potassium
682 metasomatism in sedimentary rocks and paleosols, with implications for paleoweathering
683 conditions and provenance: Geology, v. 23, p. 921–924.
684 Fildani, A., Hessler, A. M., Mason, C. C., McKay, M. P., and Stockli, D. F., 2018, Late
685 Pleistocene glacial transitions in North America altered major river drainages, as revealed
686 by deep-sea sediment: Scientific Reports, v. 8, no. 1, p. 13839. doi:10.1038/s41598-018-
687 32268-7.

688 Fildani, A., McKay, M. P., Stockli, D., Clark, J., Dykstra, M., Stockli, L., and Hessler, A., 2016,
689 The ancestral Mississippi drainage archived in the late Wisconsin Mississippi deep-sea
690 fan: Geology, v. 44, no. 6, p. 479-482. doi:10.1130/G37657.1.
691 Fisk, H., 1947, Geology of the Mississippi Valley Region: Tulsa Geological Society Digest, v.
692 15, p. 50-55.
693 Galbraith, R. F., and Roberts, R. G., 2012, Statistical aspects of equivalent dose and error
694 calculation and display in OSL dating: An overview and some recommendations:
695 Quaternary Geochronology, v. 11, p. 1-27.
696 Gehrels, G. E., 2014, Detrital Zircon U-Pb Geochronology Applied to Tectonics: Annual Review
697 of Earth and Planetary Sciences, v. 42, p. 127-149. DOI: 10.1146/annurev-earth-050212-
698 124012.
699 Ghinassi, M., Ielpi, A., Aldinucci, M., and Fustic, M., 2016, Downstream-migrating fluvial point
700 bars in the rock record: Sedimentary Geology, v. 334, p. 66-96.
701 doi:10.1016/j.sedgeo.2016.01.005.
702 Gregory, B., Herrmann, A. D., Ireland, T., and Clift, P. D., 2022, Testing the applicability of
703 zircon U-Pb dating as a provenance method in a highly altered river system, Mississippi-
704 Missouri River, USA: Basin Research, v. 34, p. 251– 273. doi:10.1111/bre.12618.
705 Grootes, P. M., and Stuiver, M., 1997, 18O/16O variability in Greenland snow and ice with 103
706 to 105 yr time resolution: Journal of Geophysical Research, v. 102, p. 26,455–426,470.
707 Gwiazda, R., Paull, C. K., Ussler, W., and Alexander, C. R., 2015, Evidence of modern fine-
708 grained sediment accumulation in the Monterey Fan from measurements of the pesticide
709 DDT and its metabolites: Marine Geology, v. 363, p. 125-133.
710 doi:10.1016/j.margeo.2015.02.006.
711 Heimann, D. C., Sprague, L. A., and Blevins, D. W., 2011, Trends in suspended-sediment loads
712 and concentrations in the Mississippi River Basin, 1950-2009, US Department of the
713 Interior, US Geological Survey.
714 Herman, F., and Champagnac, J.-D., 2016, Plio-Pleistocene increase of erosion rates in mountain
715 belts in response to climate change: Terra Nova, v. 28, no. 1, p. 2–10.
716 doi:10.1111/ter.12186.
717 Herron, M. M., 1988, Geochemical classification of terrigenous sands and shales from core or
718 log data: Journal of Sedimentary Petrology, v. 58, p. 820–829. doi:10.1306/212F8E77-
719 2B24-11D7-8648000102C1865D.
720 Hessler, A. M., and Fildani, A., 2019, Deep-sea fans: tapping into Earth's changing landscapes:
721 Journal of Sedimentary Research, v. 89, no. 11, p. 1171-1179. doi:10.2110/jsr.2019.64.
722 Hu, D., Clift, P. D., Böning, P., Hannigan, R., Hillier, S., Blusztajn, J., Wang, S., and Fuller, D.
723 Q., 2013, Holocene evolution in weathering and erosion patterns in the Pearl River delta:
724 Geochemistry Geophysics Geosystems, v. 14. doi:10.1002/ggge.20166.
725 Hülse, P., and Bentley Sr, S. J., 2012, A 210Pb sediment budget and granulometric record of
726 sediment fluxes in a subarctic deltaic system: the Great Whale River, Canada: Estuarine,
727 Coastal and Shelf Science, v. 109, p. 41-52. doi:10.1016/j.ecss.2012.05.019
728 Huntington, K. W., Blythe, A. E., and Hodges, K. V., 2006, Climate change and late Pliocene
729 acceleration of erosion in the Himalaya: Earth and Planetary Science Letters, v. 252, no.
730 1-2, p. 107-118.
731 Iizuka, T., Hirata, T., Komiya, T., Rino, S., Katayama, I., Motoki, A., and Maruyama, S., 2005,
732 U-Pb and Lu-Hf isotope systematics of zircons from the Mississippi River sand:

733 Implications for reworking and growth of continental crust: Geology, v. 33, no. 6, p. 485-
734 488.
735 Jackson, S. T., Webb, R. S., Anderson, K. H., Overpeck, J. T., Webb Iii, T., Williams, J. W., and
736 Hansen, B. C. S., 2000, Vegetation and environment in Eastern North America during the
737 Last Glacial Maximum: Quaternary Science Reviews, v. 19, no. 6, p. 489-508.
738 doi:10.1016/S0277-3791(99)00093-1.
739 Jerolmack, D. J., and Paola, C., 2010, Shredding of environmental signals by sediment transport:
740 Geophysical Research Letters, v. 37, no. 19. doi:10.1029/2010GL044638.
741 Jung, B.-J., Lee, H.-J., Jeong, J.-J., Owen, J., Kim, B., Meusburger, K., Alewell, C., Gebauer, G.,
742 Shope, C., and Park, J.-H., 2012, Storm pulses and varying sources of hydrologic carbon
743 export from a mountainous watershed: Journal of Hydrology, v. 440-441, p. 90-101.
744 doi:10.1016/j.jhydrol.2012.03.030.
745 Koi, T., Hotta, N., Ishigaki, I., Matuzaki, N., Uchiyama, Y., and Suzuki, M., 2008, Prolonged
746 impact of earthquake-induced landslides on sediment yield in a mountain watershed: The
747 Tanzawa region, Japan: Geomorphology, v. 101, no. 4, p. 692-702.
748 doi:10.1016/j.geomorph.2008.03.007.
749 Laskowski, A. K., DeCelles, P. G., and Gehrels, G. E., 2013, Detrital zircon geochronology of
750 Cordilleran retroarc foreland basin strata, western North America: Tectonics, v. 32, no. 5,
751 p. 1027-1048. doi:10.1002/tect.20065.
752 Lawton, T. F., Juárez-Arriaga, E., Ocampo-Díaz, Y. Z. E., Beltran-Triviño, A., Martens, U., and
753 Stockli, D. F., 2016, Evolution of Late Cretaceous–Paleogene foreland sediment-
754 dispersal systems of northern and central Mexico, *in* Lowery, C., ed., Mesozoic of the
755 Gulf rim and beyond: New progress in science and exploration of the Gulf of Mexico
756 basin. 35th Annual GCSSEPM Foundation Perkins-Rosen Research Conference, Gulf
757 Coast Societies SEPM (Society for Sedimentary Geology), p. 286-308.
758 Lothrop, J. C., Lowery, D. L., Spiess, A. E., and Ellis, C. J., 2016, Early Human Settlement of
759 Northeastern North America: PaleoAmerica, v. 2, no. 3, p. 192-251.
760 doi:10.1080/20555563.2016.1212178.
761 Lupker, M., France-Lanord, C., Galy, V., Lave, J., Gaillardet, J., Gajured, A. P., Guilmette, C.,
762 Rahman, M., Singh, S. K., and Sinha, R., 2012, Predominant floodplain over mountain
763 weathering of Himalayan sediments (Ganga basin): Geochimica et Cosmochimica Acta,
764 v. 84, p. 410-432.
765 Marshall, S. J., James, T. S., and Clarke, G. K. C., 2002, North American Ice Sheet
766 reconstructions at the Last Glacial Maximum: Quaternary Science Reviews, v. 21, no. 1,
767 p. 175-192. doi:10.1016/S0277-3791(01)00089-0.
768 Mason, C. C., Fildani, A., Gerber, T., Blum, M. D., Clark, J. D., and Dykstra, M., 2017, Climatic
769 and anthropogenic influences on sediment mixing in the Mississippi source-to-sink
770 system using detrital zircons: Late Pleistocene to recent: Earth and Planetary Science
771 Letters, v. 466, p. 70-79. doi:10.1016/j.epsl.2017.03.001.
772 Mason, C. C., Romans, B. W., Stockli, D. F., Mapes, R. W., and Fildani, A., 2019, Detrital
773 zircons reveal sea-level and hydroclimate controls on Amazon River to deep-sea fan
774 sediment transfer: Geology, v. 47, no. 6, p. 563-567. doi:10.1130/g45852.1.
775 Meade, R. H., and Moody, J. A., 2010, Causes for the decline of suspended-sediment discharge
776 in the Mississippi River system, 1940–2007: Hydrological Processes, v. 24, no. 1, p. 35-
777 49. doi:10.1002/hyp.7477.

778 Mertes, L. A. K., Dunne, T., and Martinelli, L. A., 1996, Channel-floodplain geomorphology
779 along the Solimões-Amazon River, Brazil: GSA Bulletin, v. 108, no. 9, p. 1089-1107.
780 doi:10.1130/0016-7606(1996)108<1089:Cfgats>2.3.Co;2.
781 Miall, A. D., 1985, Architectural-element analysis: A new method of facies analysis applied to
782 fluvial deposits: Earth-Science Reviews, v. 22, no. 4, p. 261-308. doi:10.1016/0012-
783 8252(85)90001-7.
784 Montgomery, D. R., 2007a, Dirt: The erosion of civilizations, Berkeley, University of California
785 Press, 285 p.:
786 Montgomery, D. R., 2007b, Soil erosion and agricultural sustainability: Proceedings of the
787 National Academy of Sciences, v. 104, no. 33, p. 13268-13272.
788 doi:10.1073/pnas.0611508104.
789 Murray, A. S., and Wintle, A. G., 2000, Luminescence dating of quartz using an improved
790 single-aliquot regenerative-dose protocol: Radiation measurements, v. 32, no. 1, p. 57-73.
791 doi:10.1016/S1350-4487(99)00253-X.
792 Oster, J. L., Warken, S. F., Sekhon, N., Arienzo, M. M., and Lachniet, M., 2019, Speleothem
793 paleoclimatology for the caribbean, Central America, and north America: Quaternary, v.
794 2, no. 1, p. 5. doi:10.3390/quat2010005.
795 Paola, C., Heller, P. L., and Angevine, C. L., 1992, The large-scale dynamics of grain-size
796 variation in alluvial basins, 1: Theory: Basin Research, v. 4, no. 2, p. 73-90.
797 doi:10.1111/j.1365-2117.1992.tb00145.x.
798 Pearce, A. J., and Watson, A. J., 1986, Effects of earthquake-induced landslides on sediment
799 budget and transport over a 50-yr period: Geology, v. 14, no. 1, p. 52-55.
800 doi:10.1130/0091-7613(1986)14<52:Eoelos>2.0.Co;2.
801 Pullen, A., Ibanez-Mejıa, M., Gehrels, G. E., Ibanez-Mejıa, J. C., and Pecha, M., 2014, What
802 happens when n¼ 1000? Creating large-n geochronological datasets with LA-ICP-MS for
803 geologic investigations: Journal of Analytical Atomic Spectrometry, v. 29, p. 971-980.
804 doi:10.1039/c4ja00024b.
805 Quirk, B. J., Mackey, G. N., Fernandez, D. P., Armstrong, A., and Moore, J. R., 2020,
806 Speleothem and glacier records of latest Pleistocene–early Holocene climate change in
807 the western North American interior: Journal of Quaternary Science, v. 35, no. 6, p. 776-
808 790. doi:10.1002/jqs.3221.
809 Rhodes, E., 2011, Optically Stimulated Luminescence Dating of Sediments over the Past
810 200,000 Years: Annual Review of Earth and Planetary Sciences, v. 39, p. 461-488.
811 doi:10.1146/annurev-earth-040610-133425.
812 Rittenour, T. M., 2018, Dates and Rates of Earth-Surface Processes Revealed using
813 Luminescence Dating: Elements, v. 14, no. 1, p. 21-26. doi:10.2138/gselements.14.1.21.
814 Romans, B. W., Castelltort, S., Covault, J. A., Fildani, A., and Walsh, J. P., 2016, Environmental
815 signal propagation in sedimentary systems across timescales: Earth-Science Reviews, v.
816 153, p. 7–29. doi:10.1016/j.earscirev.2015.07.012.
817 Saucier, R. T., 1969, Geological Investigation of the Mississippi River area, Artonish to
818 Donaldsonville, LA: U.S. Army Corps of Engineers.
819 Singh, M., Sharma, M., and Tobschall, H. J., 2005, Weathering of the Ganga alluvial plain,
820 northern India: implications from fluvial geochemistry of the Gomati River: Applied
821 Geochemistry, v. 20, p. 1-21.
822 Smith, D. G., 1987, Meandering river point bar lithofacies models: modern and ancient examples
823 compared, *in* Ethridge, F. G., Flores, R. M., and Harvey, M. D., eds., Recent

Developments in Fluvial Sedimentology, Volume 39, The Society of Economic Paleontologists and Mineralogists (SEPM), p. 83-93.
Sternberg, H. O. R., 1956, A Contribution to the Geomorphology of the False River Area, Louisiana [PhD PhD]: Louisiana State University, 181 p.
Sundell, K., and Saylor, J. E., 2017, Unmixing detrital geochronology age distributions: Geochemistry Geophysics Geosystems, v. 18, p. 2872–2886.
Syvitski, J. P. M., C., V., Kettner, A. J., and Green, P., 2005, Impact of humans on the flux of terrestrial sediment to the global coastal ocean: Science, v. 308, p. 376-380.
Thomas, R. G., Smith, D. G., Wood, J. M., Visser, J., Calverley-Range, E. A., and Koster, E. H., 1987, Inclined heterolithic stratification—Terminology, description, interpretation and significance: Sedimentary Geology, v. 53, no. 1, p. 123-179. doi:10.1016/S0037-0738(87)80006-4.
Thomson, K. D., Stockli, D. F., and Fildani, A., 2022, Anthropogenic impact on sediment transfer in the upper Missouri River catchment detected by detrital zircon analysis: GSA Bulletin. doi:10.1130/b36217.1.
URS Group, 2012, The History of Building Elevation in New Orleans, Federal Emergency Management Agency.
US Army Corps of Engineers, 2017, History of the Lower Mississippi Levee System: Mississippi River Commission, Mississippi Valley Division.
Vermeesch, P., 2004, How many grains are needed for a provenance study?: Earth and Planetary Science Letters, v. 224, p. 351–441.
Vermeesch, P., 2013, Multi-sample comparison of detrital age distributions: Chemical Geology, v. 341, p. 140–146. doi:10.1016/j.chemgeo.2013.01.010.
-, 2018, IsoplotR: A free and open toolbox for geochronology: Geoscience Frontiers, v. 9, no. 5, p. 1479-1493. doi:10.1016/j.gsf.2018.04.001.
Waters, M. R., 2019, Late Pleistocene exploration and settlement of the Americas by modern humans: Science, v. 365, no. 6449, p. eaat5447. doi:10.1126/science.aat5447.

Figure Captions

Figure 1. A) Shaded topographic map of North America showing the extent of the Mississippi catchment and the major tributaries that are supplying sediment to the lower reaches of the river where a sample during this work. Red line shows the approximate location of the ice front during the LGM (Marshall et al., 2002). Data is Shuttle Radar Topography Mission (SRTM) from NASA. B) Satellite image of the Mississippi River lower reaches from Google Earth, showing the sampling locations in this region.

Figure 2. LiDAR topography image of the region around False River and associated point bar showing the locations of the drilling sites from which samples were taken as part of this study. White stars show the point bar apex at the end of each accretionary phase, while pink stars show apices after the point bar has become compound in its geometry. The red lines show the major depositional units as defined by Clift et al. (2019). The dates shown are derived from OSL analysis as described in the text.

Figure 3. Tectonic map of North America showing the major crystalline blocks and their zircon U-Pb ages that comprise the continental interior and which are drained by the tributaries of the Mississippi River. Their unique geological history can be isolated in the detrital minerals eroded from them and delivered to the lower reaches. Modified after Lawton et al. (2016).

Figure 4. Cross plots of A) Silica and B) Zirconium concentrations compared to median grain size.

Figure 5. Geochemical signature of the analyzed samples illustrated by a CN-A-K ternary diagram (Fedo et al., 1995). Modern tributary data from Gregory et al. (2022). CN denotes the mole weight of Na_2O and CaO* (CaO* represent the CaO associated with silicate, excluding all the carbonate). A and K indicate the content of Al_2O_3 and K_2O respectively. Samples closer to A are rich in kaolinite, chlorite and/or gibbsite (representing by kao, chl and gib). CIA values are also calculated and shown on the left side, with its values are correlated with the CN-A-K. Abbreviations: sm (smectite), pl (plagioclase), ksp (K-feldspar), il (illite), m (muscovite). Numbers in italics indicate deposition time in years ago.

Figure 6. Kernel density estimate (KDE) diagrams showing the age distribution of detrital zircon grains in the different sediment sample is considered in the study. Bandwidth 15 m.y. Colored vertical bars show age ranges that have significance for sediment provenance and relate to the different tectonic blocks shown in Figure 3. Sampling month for the modern samples is shown under the sample number.

Figure 7. Plots showing the relationship between provenance-sensitive population groups and median grain size for the samples. The plot shows no clear relationship between grain size and zircon age spectra.

Figure 8. Two-dimensional multidimensional scalar diagram (MDS) comparing the age spectra of the detrital zircon from the different samples considered in the study. Note that two of the modern samples are quite distinct from the other recent deposits and that the modern samples

cluster separately from the majority of samples taken from the False River Point Bar. Note the similarity of the Ohio River with most of the samples. Modern tributary data from Gregory et al. (2022).

Figure 9. Summary of the unmixing calculations as plotted against depositional age showing the varying contribution from four contrasting source terrains of the Superior Province, Appalachian Mountains, Rocky Mountain foreland and Yavapai-Mazatal. We compare the erosion history with climate variability as shown by the Greenland ice core (GISP2) from Grootes et al. (1997). Clas = Classic, Woodld = Woodland.

Figure 10. Schematic representation of the how erosion and landscape in the Mississippi River basin has evolved since the LGM. A) LGM, with dominant sediment supply from reworked glaciers in the north. B) Late Holocene, with more erosion in the Appalachians linked to wetter climate and start of agriculture buffered by floodplain storage and reworking. C) Modern river, with little buffering in the lower reaches, reduced erosion from the Appalachians and more erosion from the Rocky Mountain foreland.

Table Captions

Table 1. List of the sample locations and depth in the core sites where appropriate for the materials used in this study.

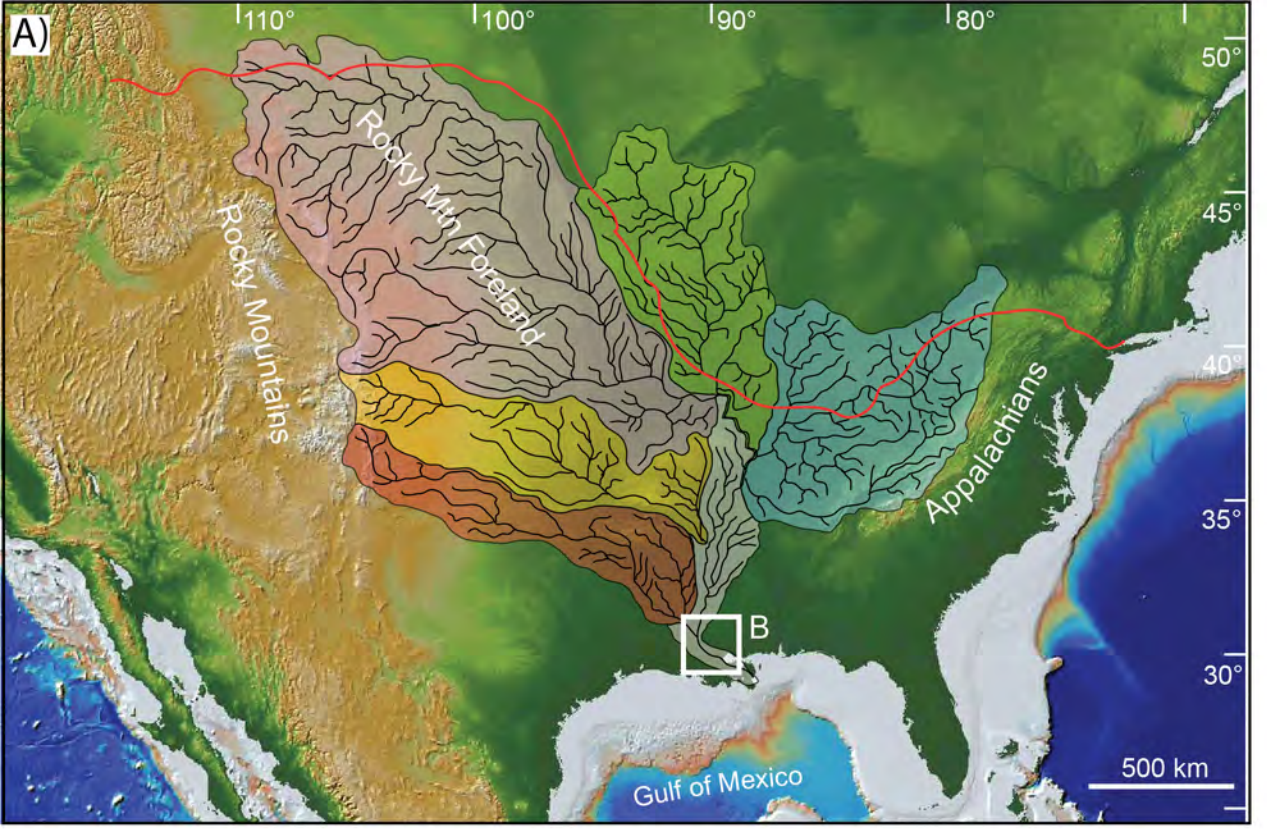

Missouri River
Upper Mississippi River
Red River
Arkansas River
Ohio River
Lower Mississippi River

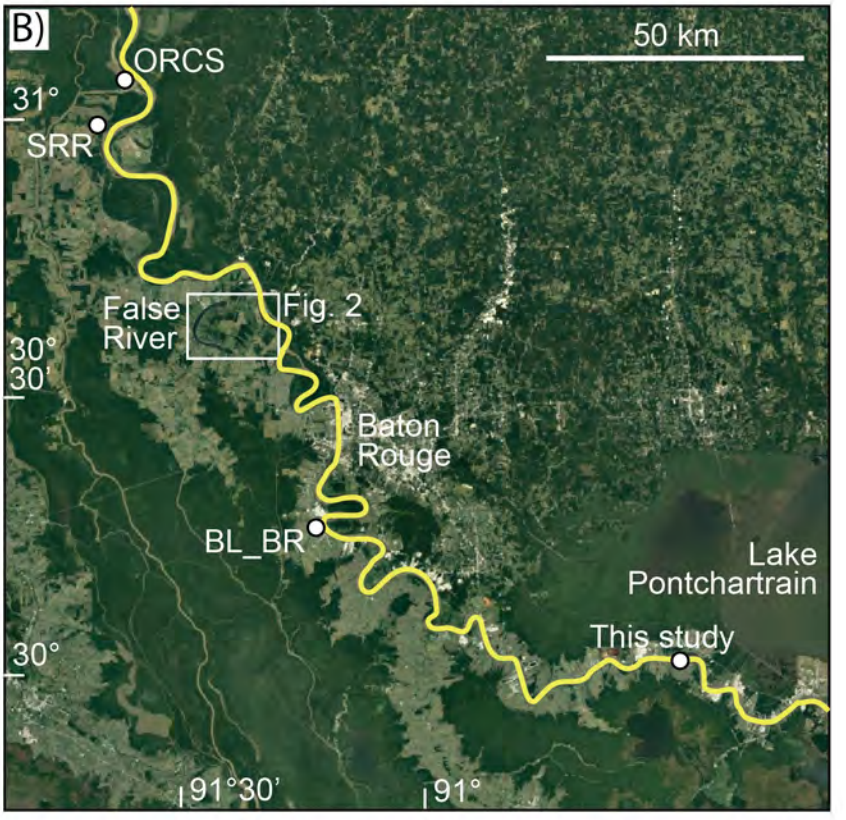

Figure 1
Neubeck et al.

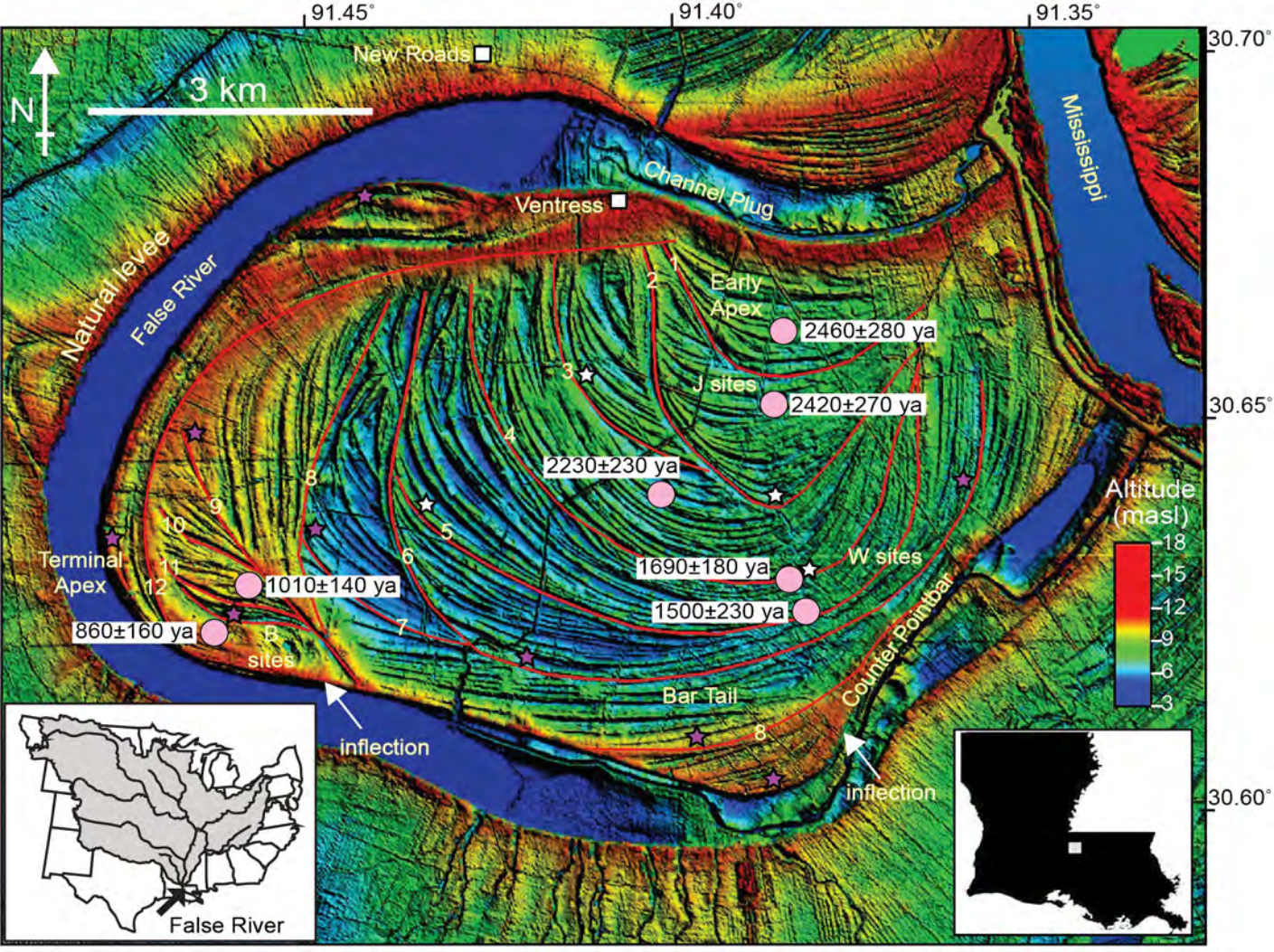

Figure 2
Neubeck et al.

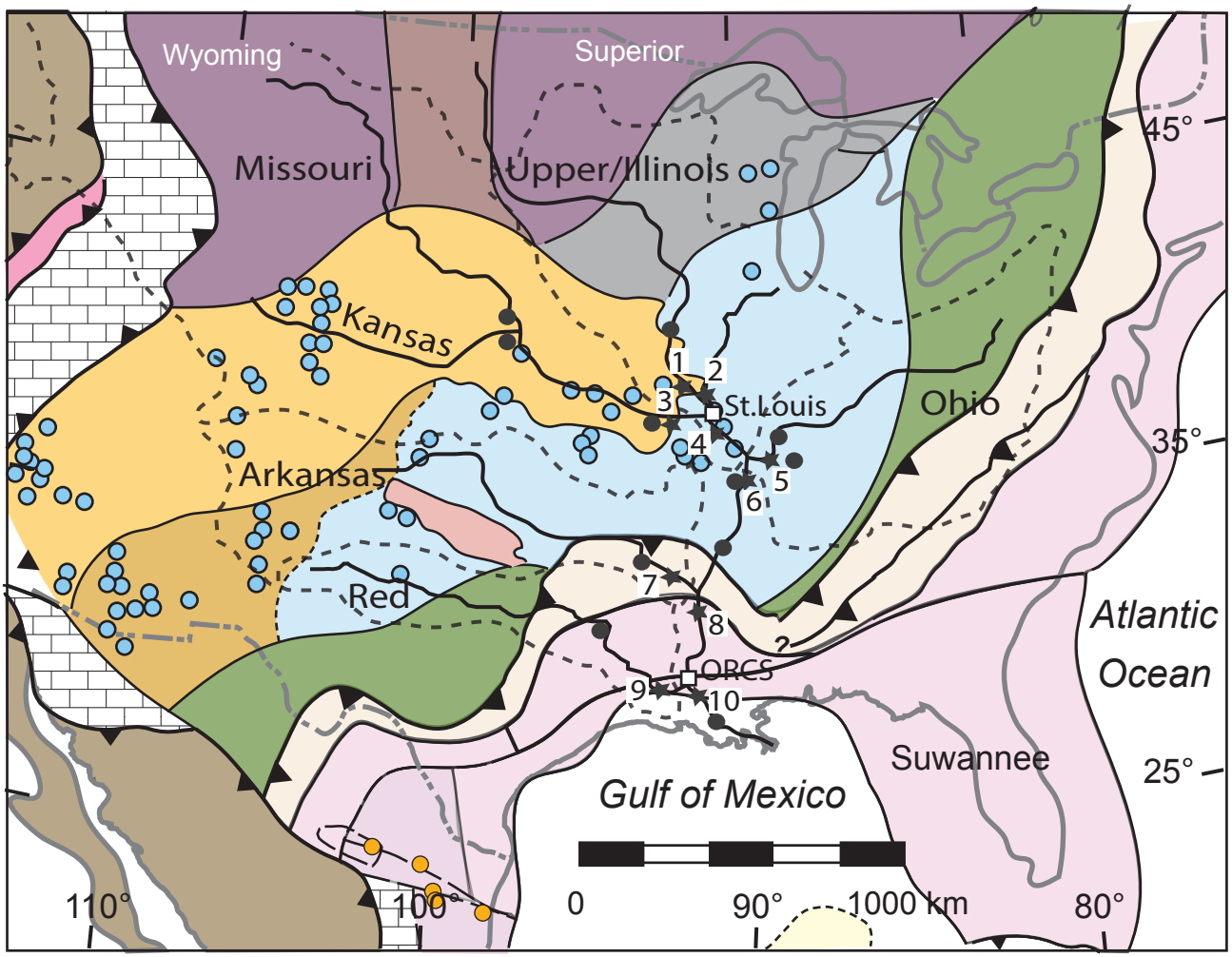

1.48-1.34 Ga granites

Permo-Triassic granites ~285-245 Ma; "E. Mexico arc"

Gregory et al. (2021)

Mason et al. (2017)

ORCS = River Control Structure
WLD = Wax Lake Delta

Cordilleran terranes

Roberts Mountain Allochthon

Miogeocline

Appalachian 380-500 Ma

Peri-Gondwana (incl. Suwannee) 500-650 Ma

Grenville 1000-1200 Ma

Granite Rhyolite ~1320-1480 Ma

Yavapai 1600-1700 Ma

Mazatzal 1650-1800 Ma

Sabine Block 1600-1800 Ma

Penokean 1800-1900 Ma

Trans Hudson 1800-1900 Ma

Superior 2500-2700 Ma

Figure 3
Neubeck et al.

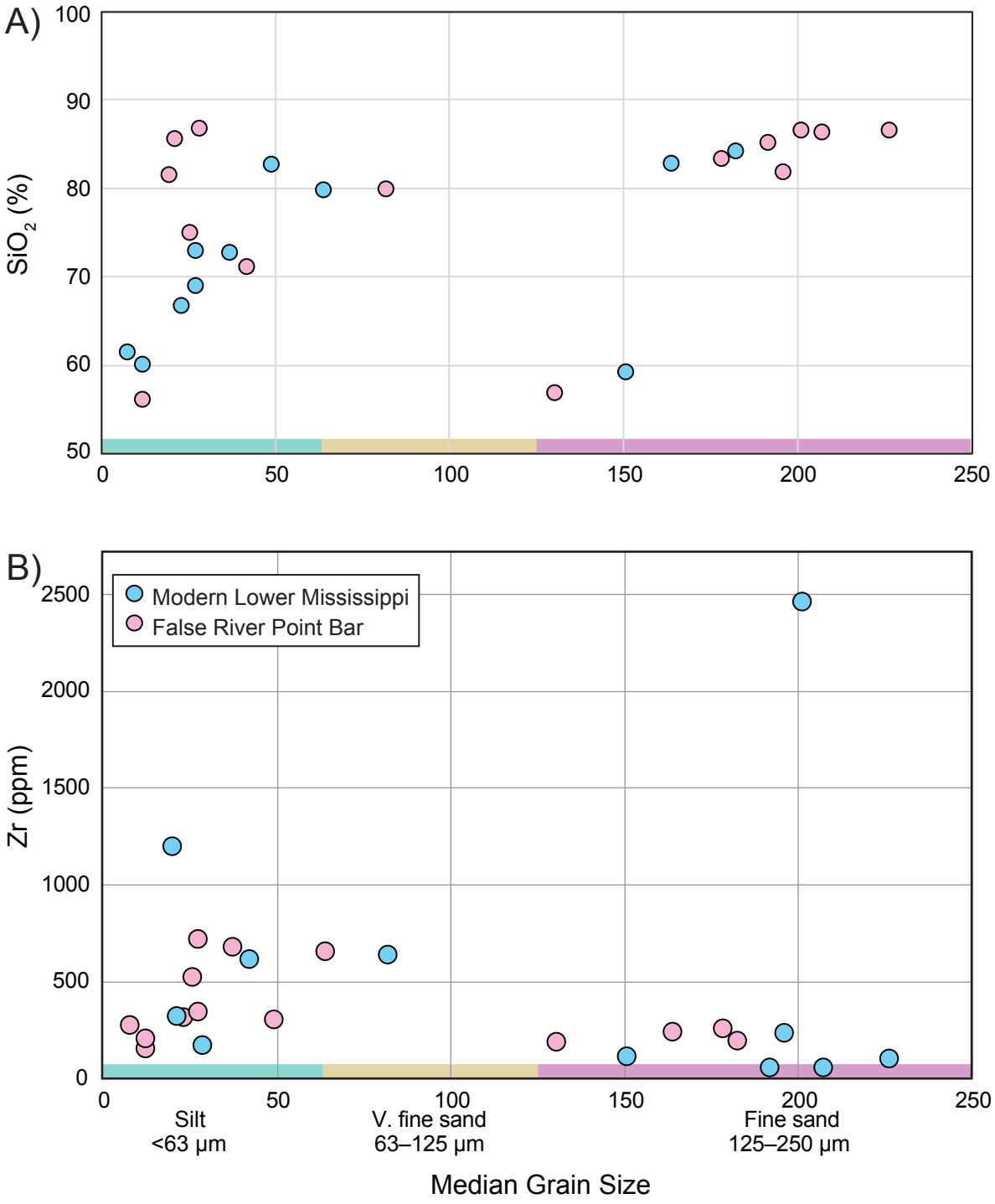

Figure 4
Neubeck et al.

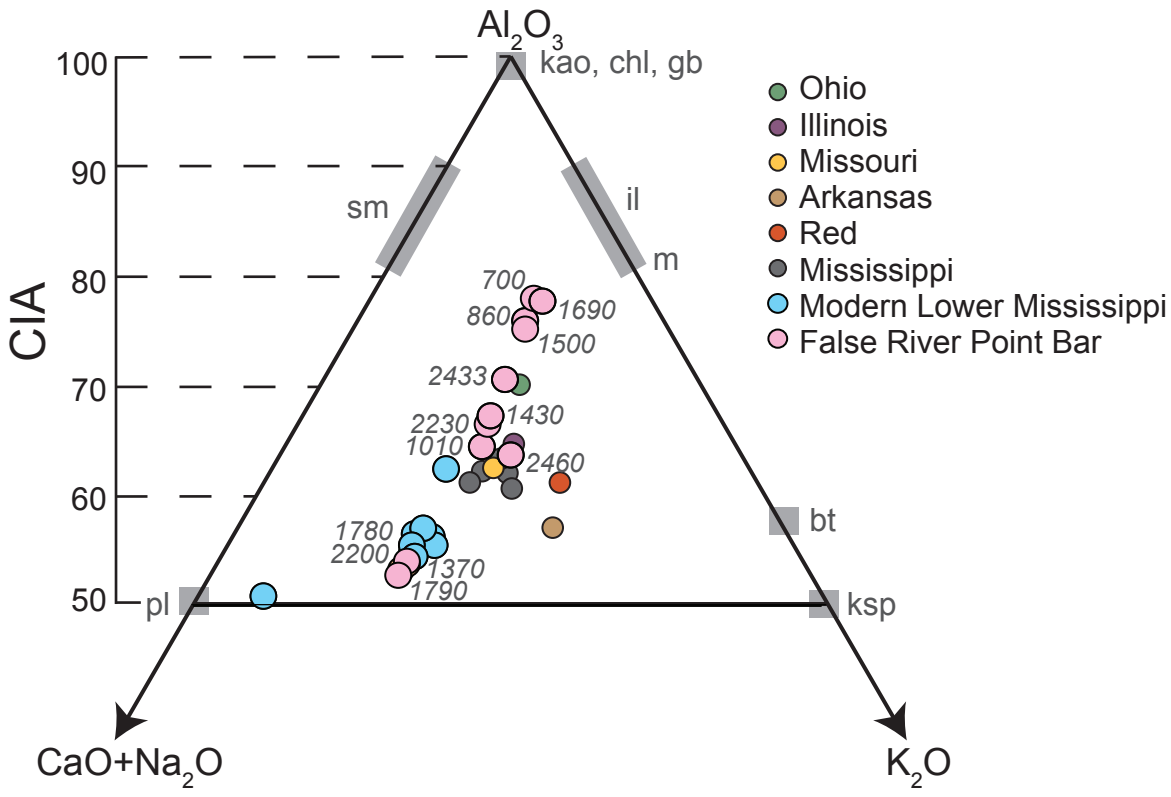

Figure 5
Neubeck et al.

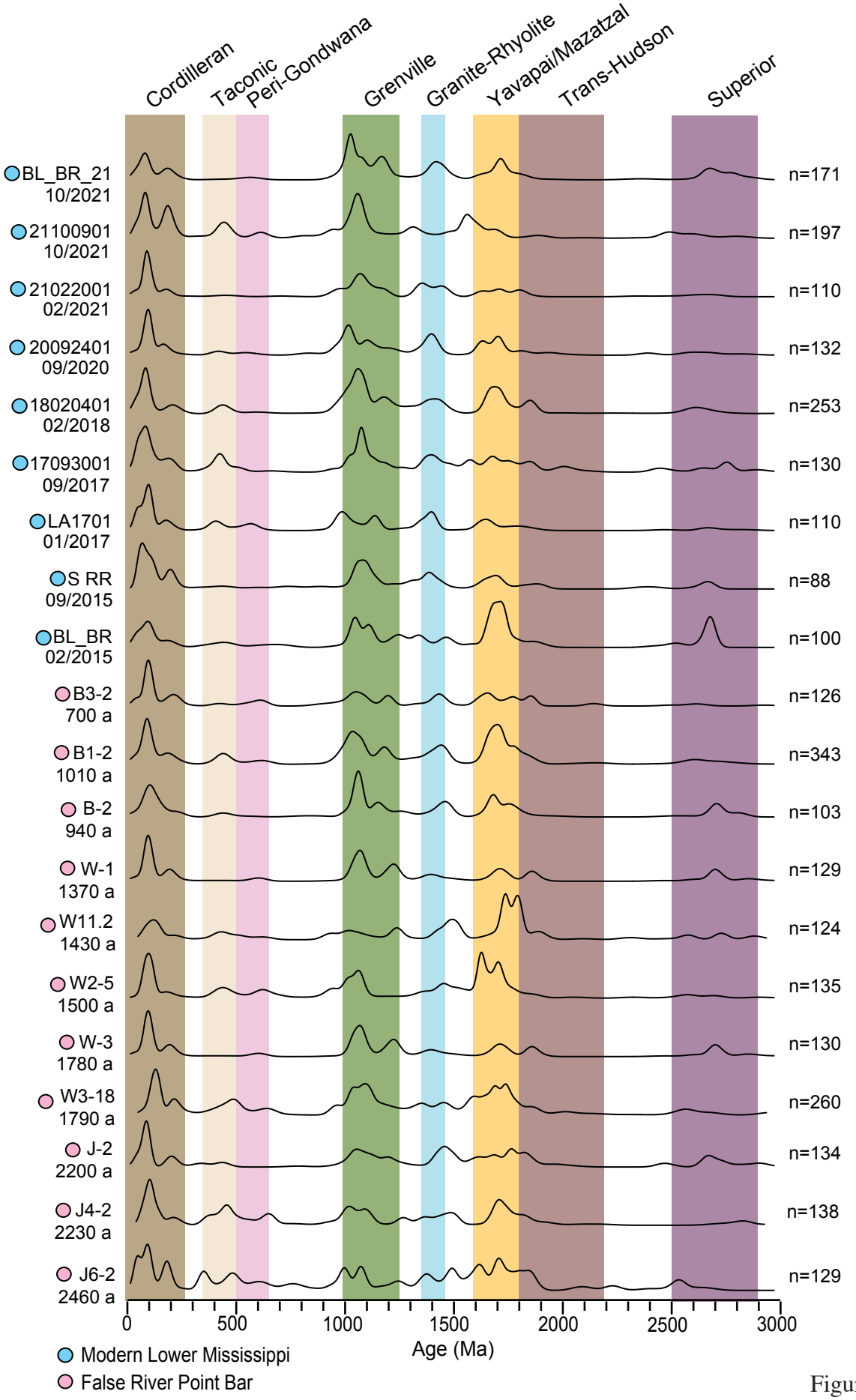

Figure 6
Neubeck et al.

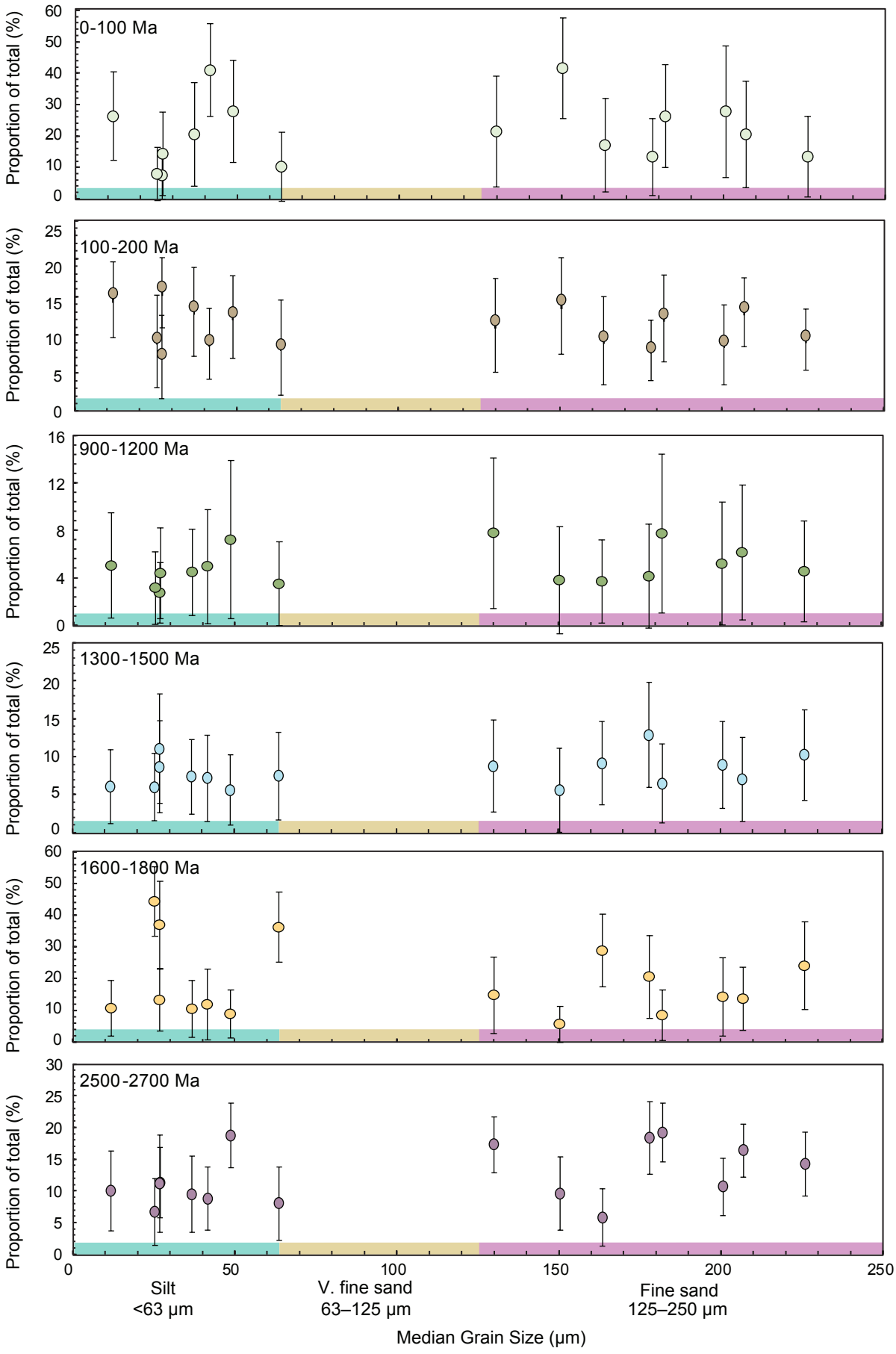

Figure 7
Neubeck et al.

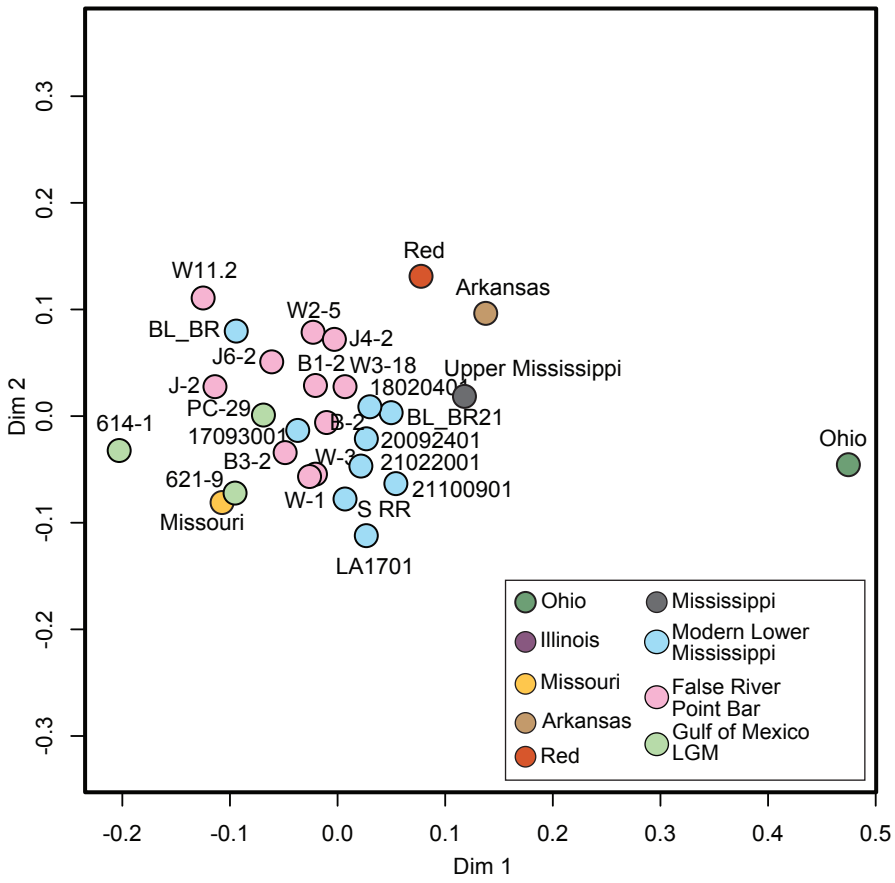

Figure 8
Neubeck et al.

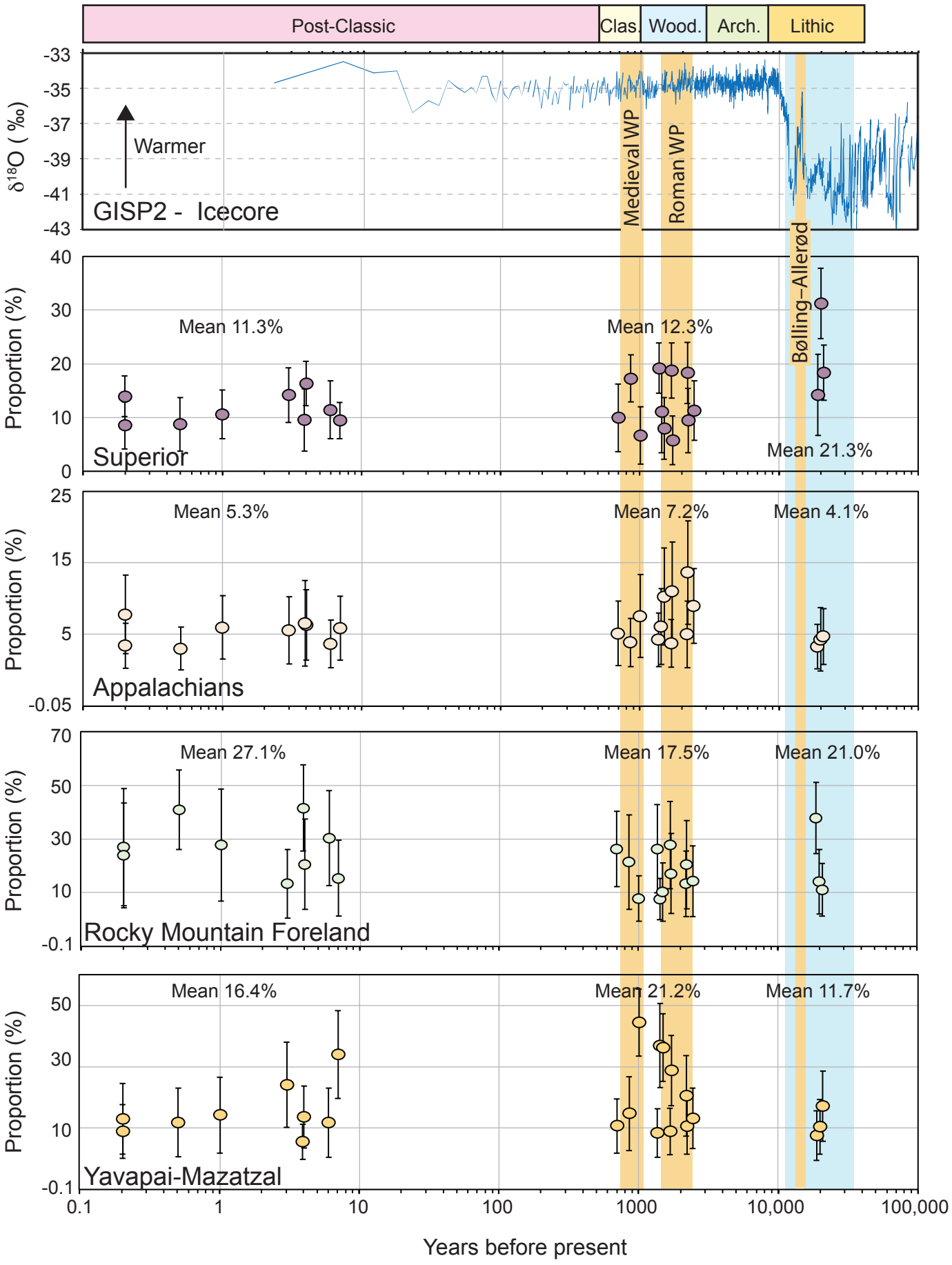

Figure 9
Neubeck et al.

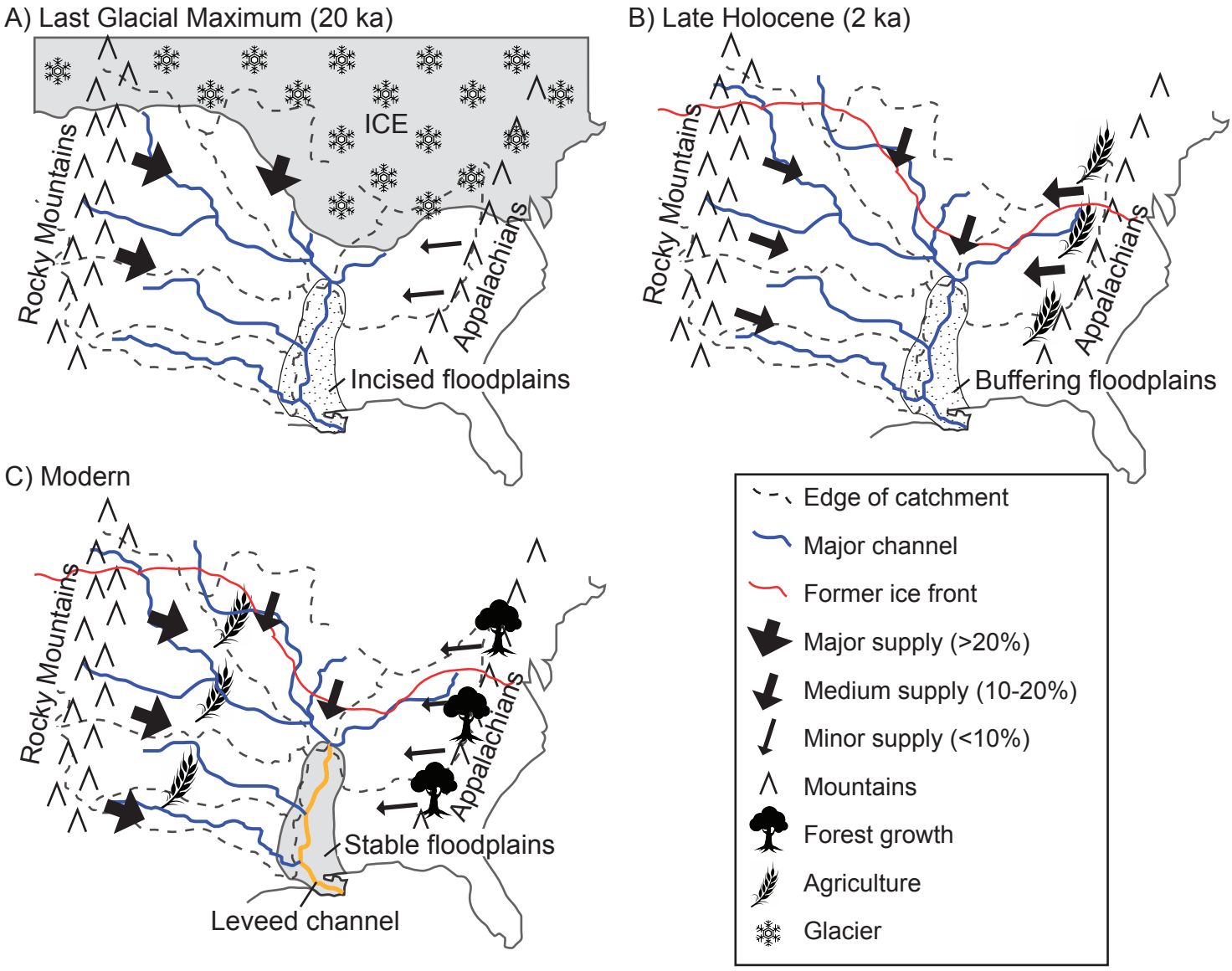

Figure 10
Neubeck et al.

Table 1

Sample	Depth (m)	Date collected	Depositional age (a)	Sediment type	North (°)	West (°)	Zircon	OSL
21100901	0	9-Oct-21	0.3	Fine sand	30.053060	90.555560	X	
BLBR21	0	9-Oct-21	0.3	Silt	30.297220	91.227500	X	
21022001	0	20-Feb-21	0.8	Silt	30.053060	90.555560	X	
21012501	0	25-Jan-21	0.9	Fine sand	30.053060	90.555560	X	
20121501	0	15-Dec-20	1.0	Fine sand	30.053060	90.555560	X	
20110101	0	10-Nov-20	1.1	Silt-Fine Sand	30.053060	90.555560	X	
20092401	0	9-Sep-20	1.3	Fine sand	30.053060	90.555560	X	
18020401	0	4-Feb-18	4	Fine sand	30.053060	90.555560	X	
LA1701	0	1-Sep-17	4.8	Fine sand	30.053060	90.555560	X	
17093001	0	3-Sep-17	4.8	Fine sand	30.053060	90.555560	X	
B3-2	3.0	5-Oct-20	700	Silt	30.628333	91.466389	X	X
B2-14, B2-16	15.8-19.5	9-Feb-17	860	Fine sand	30.630500	91.464317	X	
B2-2	3.0	5-Oct-20	940	Silt	30.630278	91.465278		
B1-2	3.0	5-Oct-20	1010	Silt	30.632500	91.463889	X	X
W1-17, W1-18	19.5-21.9	11-Feb-17	1370	Med sand	30.624750	91.384172	X	
W11-2	3.0	5-Oct-20	1430	Fine sand	30.625680	91.387940	X	
W2-5	4.9-6.1	12-Feb-17	1500	Silt-Fine Sand	30.627569	91.387664	X	
W10-2	3.0	5-Oct-20	1500	Silt	30.627570	91.390230	X	X
W9-2	3.0	5-Oct-20	1690	Silt	30.630530	91.394500	X	X
W3-10, W3-11	10.9-13.4	13-Feb-17	1780	Med sand	30.632081	91.394200	X	
W3-18	21.3	13-Feb-17	1790	Fine sand	30.632081	91.394200	X	
J2-11, J2-10	12.8	1-Feb-17	2200	Fine sand	30.656072	91.389936	X	
J4-2	3.0	6-Oct-20	2230	Silt	30.648460	91.407270	X	X
J7-2	3.0	6-Oct-20	2420	Silt	30.656650	91.389950		X
J5-2	3.0	6-Oct-20	2433	Silt	30.658980	91.389670	X	
J6-2	3.0	6-Oct-20	2460	Silt	30.664070	91.388470	X	X

921 Table 2. Optically Stimulated Luminescence Age Information. (1) Age analysis using the single-
922 aliquot regenerative-dose procedure of Murray and Wintle (2000) on 1-mm small-aliquots of
923 quartz sand. Number of aliquots used in age calculation and number of aliquots analyzed in
924 parentheses. (2) Equivalent dose (DE) calculated using the Minimum Age Model (MAM) of
925 Galbraith and Roberts (2012).
926
927 Table 3. Major element compositions of samples considered in the study as derived from XRF
928 analyses. Location datum is WGS84.
929